MRI methods for in vivo detection of microstructural tissue changes in dementia: Is what we don´t see more important than what we see?

Reinhold Schmidt
Department of Neurogeriatrics
University Clinic of Neurology
Medical University Graz, Austria

A White Matter Disorder in Dementia of the Alzheimer Type: A Pathoanatomical Study

A. Brun, MD, and E. Englund, MD

Ann Neurol 19:253–262, 1986

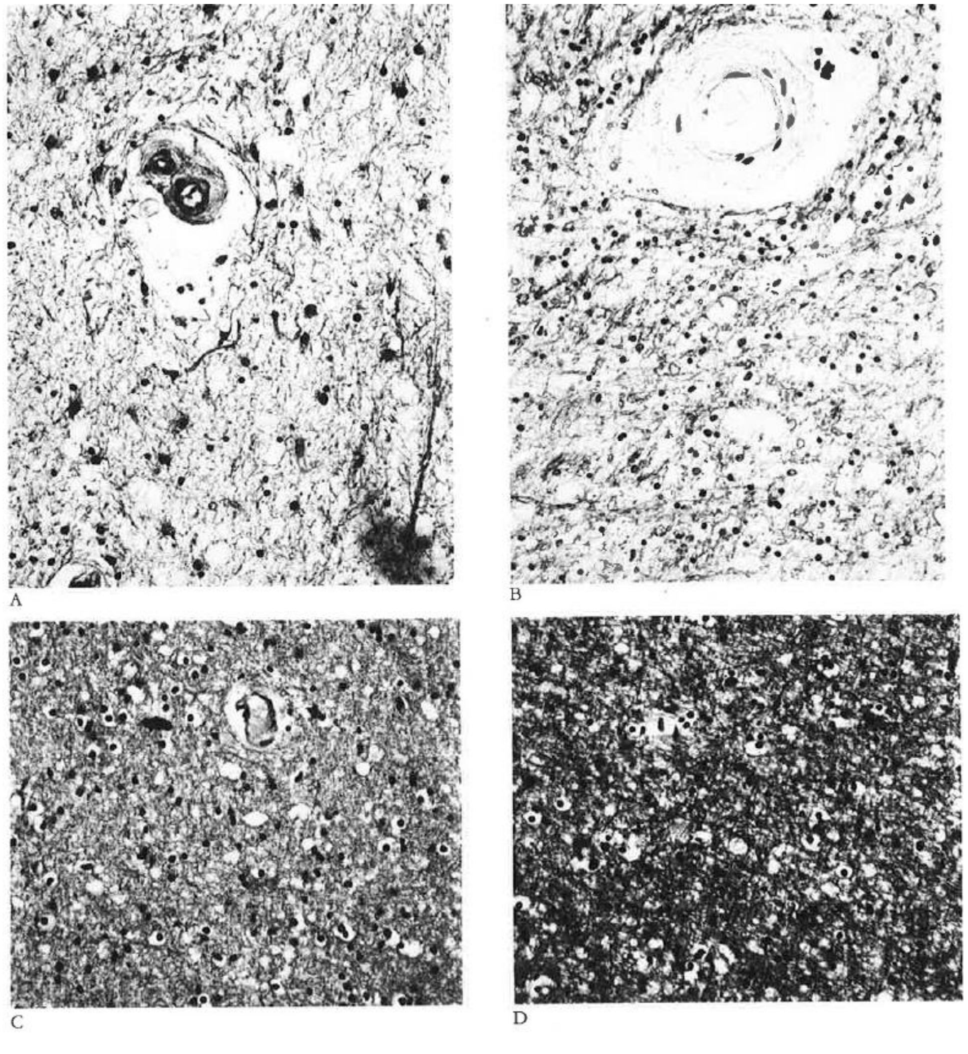

Fig 2. Frontal white matter in a patient with senile dementia of the Alzheimer type with (A, B) mild to moderate changes compared with (C, D) normal white matter. Note the attenuation of tissue with partial loss of oligodendroglial cells (A, B) and myelin sheaths (B), reactive astrogliosis (A), and a fibrohyaline arteriosclerosis (A, B). ((A, C) H&E, (B, D) Luxol fast blue; ×250.)

Promising techniques to look underneath the surface

Diffusion Tensor Imaging (DTI)

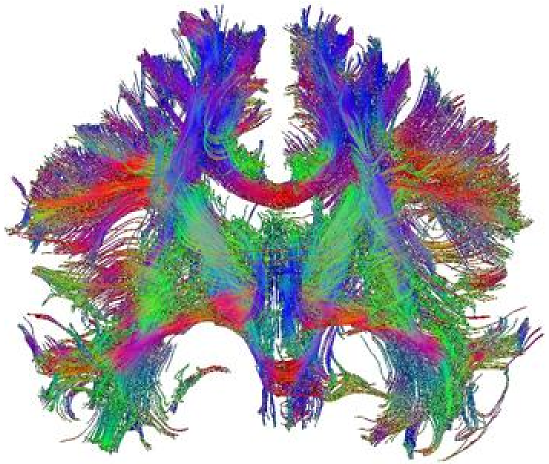

Magnetization Transfer Imaging (MTI)

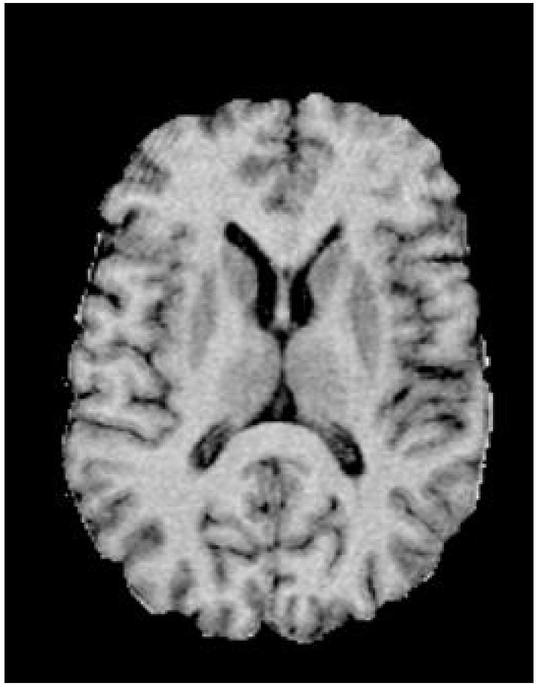

Iron Detection

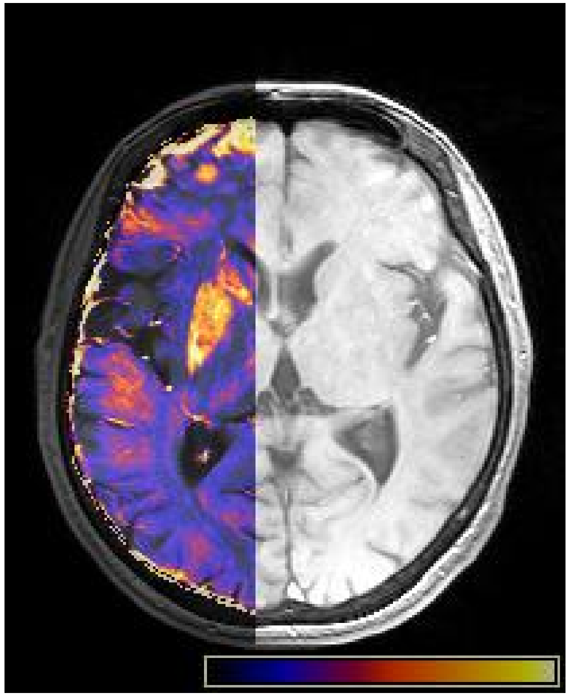

Microstructural MRI

cellular tissue composition

Magnetization transfer (MT) imaging probes magnetization exchange between tissue water and protons bound to macromolecules (myelin)

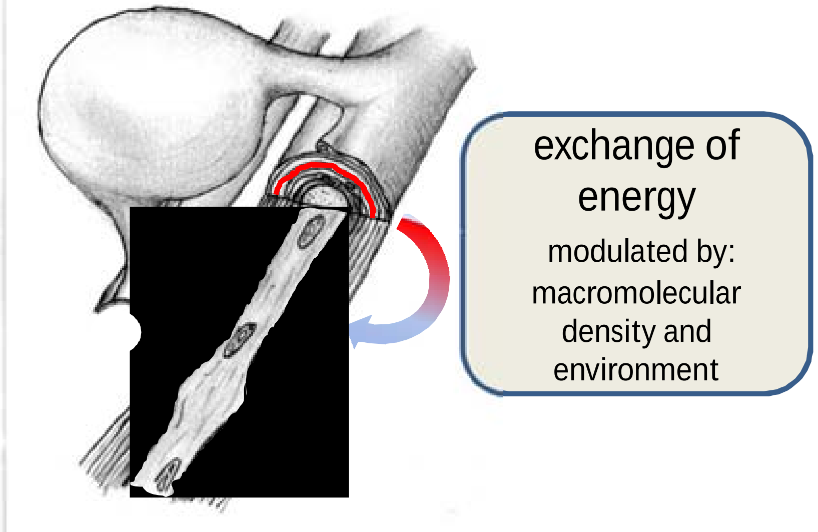

- assessed by the magnetization transfer ratio (MTR) or
- true quantitatively by qMT

Cellular organization

Diffusion tensor imaging (DTI) probes mobility of water protons in the axons

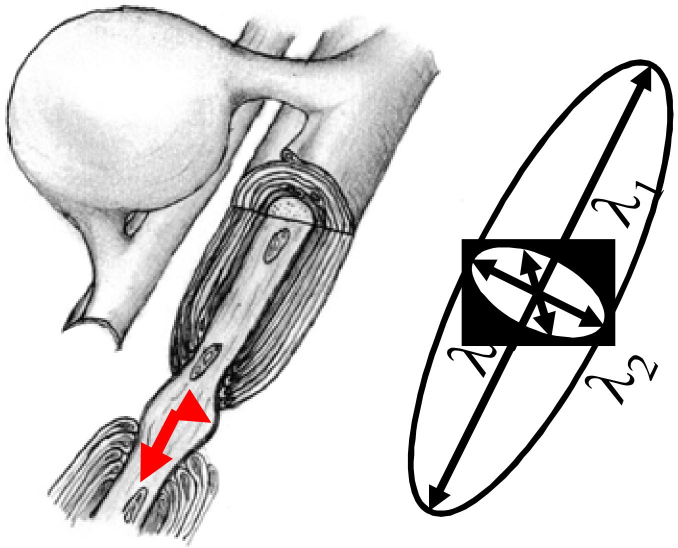

- restricted mobility in brain tissue
- modeled by a diffusion ellipsoid
- allows estimation of MD, FA, RD, AD

Diffusion Tensor Imaging

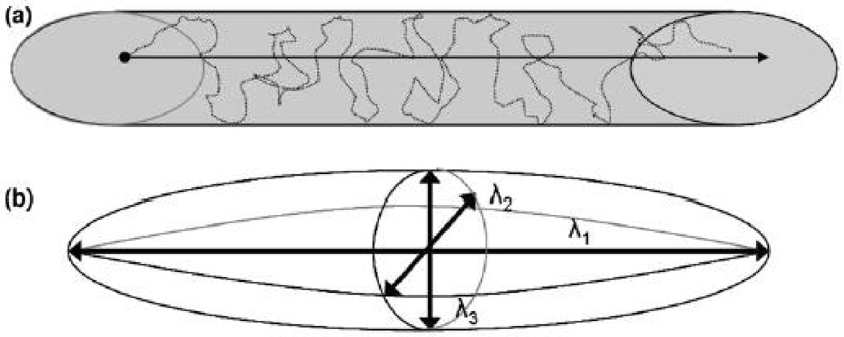

(c)

$$\hat{\lambda} = \begin{pmatrix} \lambda_1 & 0 & 0 \\ 0 & \lambda_2 & 0 \\ 0 & 0 & \lambda_3 \end{pmatrix}$$

Mean Diffusivity = $(\lambda_1+\lambda_2+\lambda_3)/3$

Fractional Anisotropy = $\sqrt{\frac{1}{2}}\frac{\sqrt{(\lambda_1-\lambda_2)^2+(\lambda_2-\lambda_3)^2+(\lambda_3-\lambda_1)^2}}{\sqrt{\lambda_1^2+\lambda_2^2+\lambda_3^2}}$

Axial (II) diffusivity = λ_1

Radial (T) diffusivity = $(\lambda_2+\lambda_3)/2$

MD = mean of all three axes of the diffusion ellipsoid and reflects the rate of water diffusion within a voxel, independently of the directionality.

FA= fraction of the tensor that can be assigned to anisotropic (directional) diffusion

Diffusion tensor imaging (DTI) probes mobility of water protons in the axons

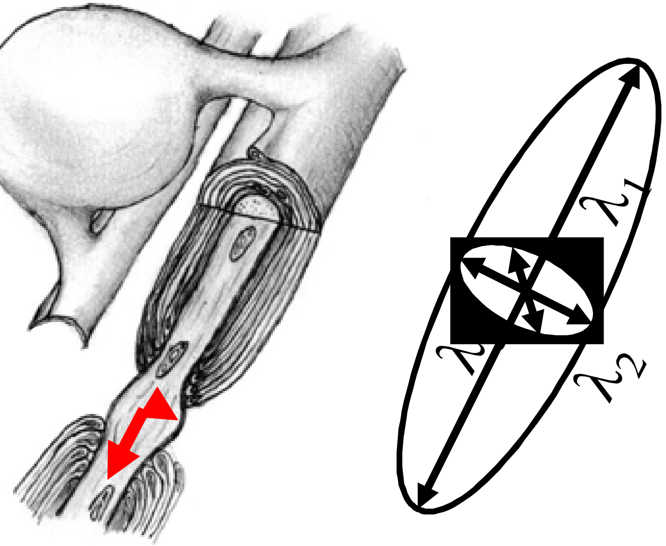

- restricted mobility in brain tissue
- modeled by a diffusion ellipsoid
- allows estimation of MD, FA, RD, AD

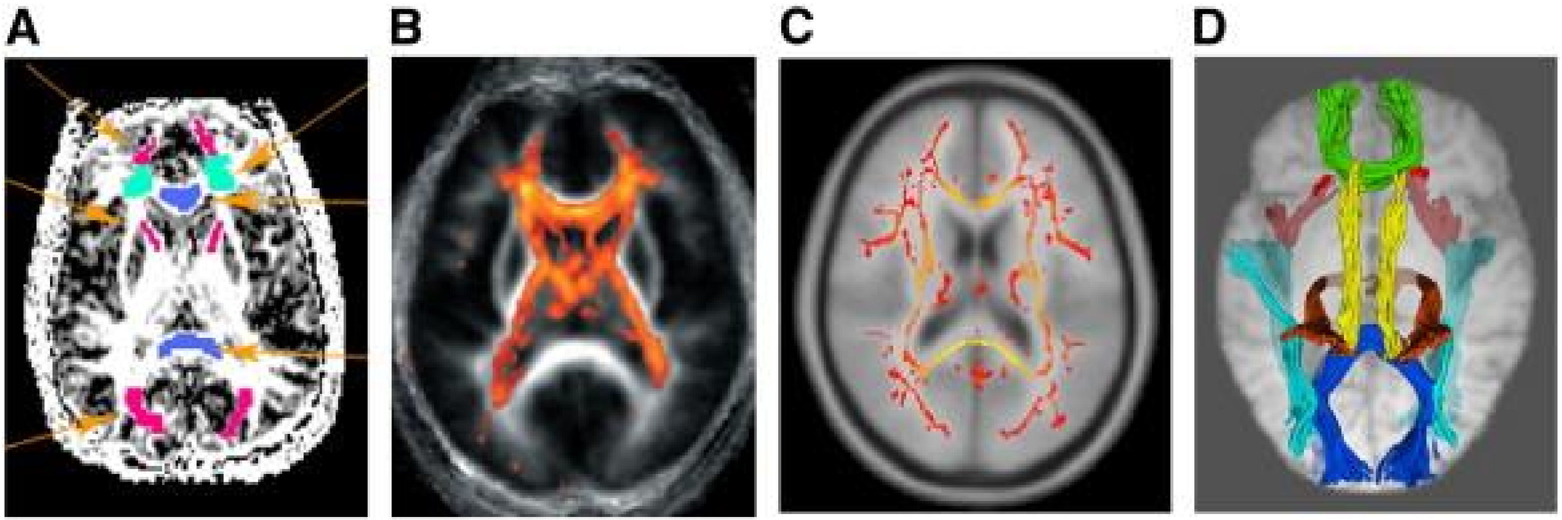

Methods for representing diffusion tensor imaging (DTI) data. A = regions of interest (in color) placed directly on DTI image; B = voxel-based morphometry (VBM); C = mean "skeleton" of white matter tracts from tract-based spatial statistics (TBSS); D = fiber tracking of white matter pathways.

David J. Madden , Ilana J. Bennett , Agnieszka Burzynska , Guy G. Potter , Nan-kuei Chen , Allen W. Song

Diffusion tensor imaging of cerebral white matter integrity in cognitive aging

Biochimica et Biophysica Acta (BBA) - Molecular Basis of Disease Volume 1822, Issue 3 2012 386 - 400

http://dx.doi.org/10.1016/j.bbadis.2011.08.003

Cross-Sectional DTI studies in Aging

Study	year	Sample Size	Findings
Charlton et al.	2010	99 HC	Increasing age associated with decrease FA and increase in MD. Working memory, executive function and speed correlated with decrease in FA and increased MD
Della et al.	2009	16 AD, 14 HC	MD correlated with executive and attention scores
Hannedottir et al	2009	60 Hypertensives	Mean MD correlated with executive function in untreated hypertensive subjects. No other significant correlations detected
Vernooj et al	2009	860 population-based	Regardless of macrostructural white matter changes, a higher mean diffusivity or higher axial and radial diffusivities within white matter lesions or normal-appearing white matter were related to worse performance on tasks assessing information processing speed and global cognition
Schmidt et al	2010	340 LADIS participants	Strong associations between the peak height of the ADC histogram of whole-brain tissue and NABT with memory performance, executive dysfunction, and speed, which remained after adjustment for WMH lesion volume and brain atrophy and were consistent among centers. No such association was seen with the mean ADC of WMH.

Diffusion-Weighted Imaging and Cognition in the Leukoariosis and Disability in the Elderly Study

Reinhold Schmidt, Stefan Ropele, José Ferro, Sofia Madureira, Ana Verdelho, Katja Petrovic, Alida Gouw, Wiesje M. van der Flier, Christian Enzinger, Leonardo Pantoni, Domenico Inzitari, Timo Erkinjuntti, Philip Scheltens, Lars O. Wahlund, Gunhild Waldemar, Egill Rostrup, Anders Wallin, Frederik Barkhof, Franz Fazekas and on behalf of the LADIS study group

Stroke 2010;41:e402-e408; originally published online Mar 4, 2010;

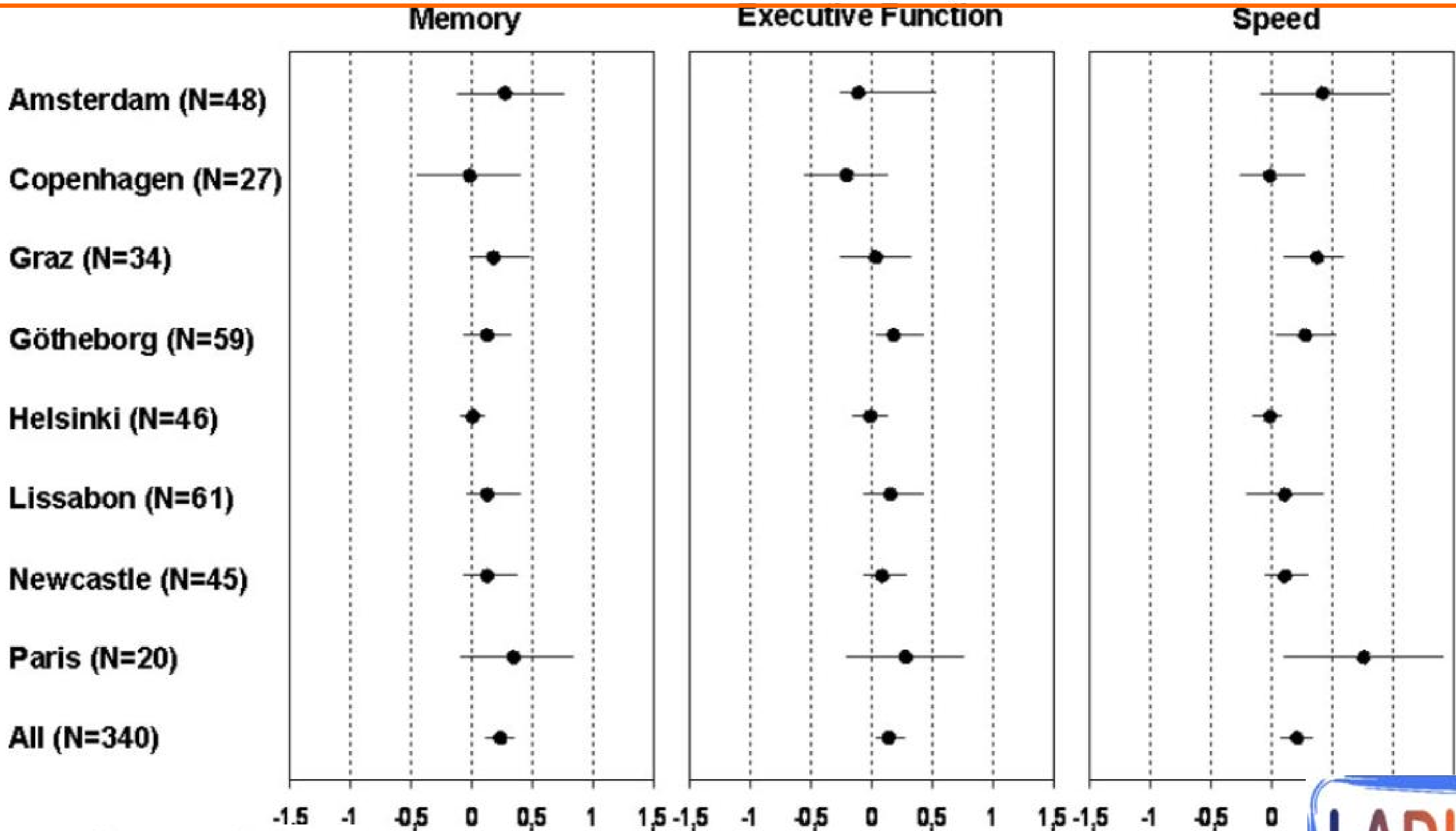

Stroke
American Stroke Association.
A Division of American Heart Association

LADIS

Cross-Sectional DTI studies in SVD

Study	year	Sample Size	Findings
O´Sullivan et al	2001	36 lacunar infarcts and SVD	Increased MD and decreased FA in the normal appearing white matter, correlated with executive function
O´Sullivan et al	2004	30 lacunar infarcts and SVD	MD in normal appearing white matter correlated with executive function and general IQ
O´Sullivan et al	2004	18 CADASIL	Increased MD and reduced FA in white matter lesion, normal appearing white matter and normal appearing grey matter (thalamus, putamen, globus pallidum) which correlated with executive dysfunction.
Chabriat et al	1999	16 CADASIL	MD higher and FA lower in lesion and normal appearing white matter compared with control. MD/FA in lesion correlated with Rankin and MMSE
O´Sullivan et al	2005	18 CADASIL	Different cognitive functions correlate with structural integrity at different sites in the white and subcortical gray matter. The distribution of regions correlating specifically with executive function provides clues to the organization of the relevant cognitive networks and their important white matter projections. The cingulum bundle is one candidate tract that may carry anteroposterior connections important for executive processes.

Damage within a network of white matter regions underlies executive dysfunction in CADASIL.
OSullivan, M; PhD, MRCP; Barrick, T; Morris, R; Clark, C; Markus, H; DM, FRCP

Neurology. 65(10):1584-1590, November 22, 2005.
DOI: 10.1212/01.wnl.0000184480.07394.fb

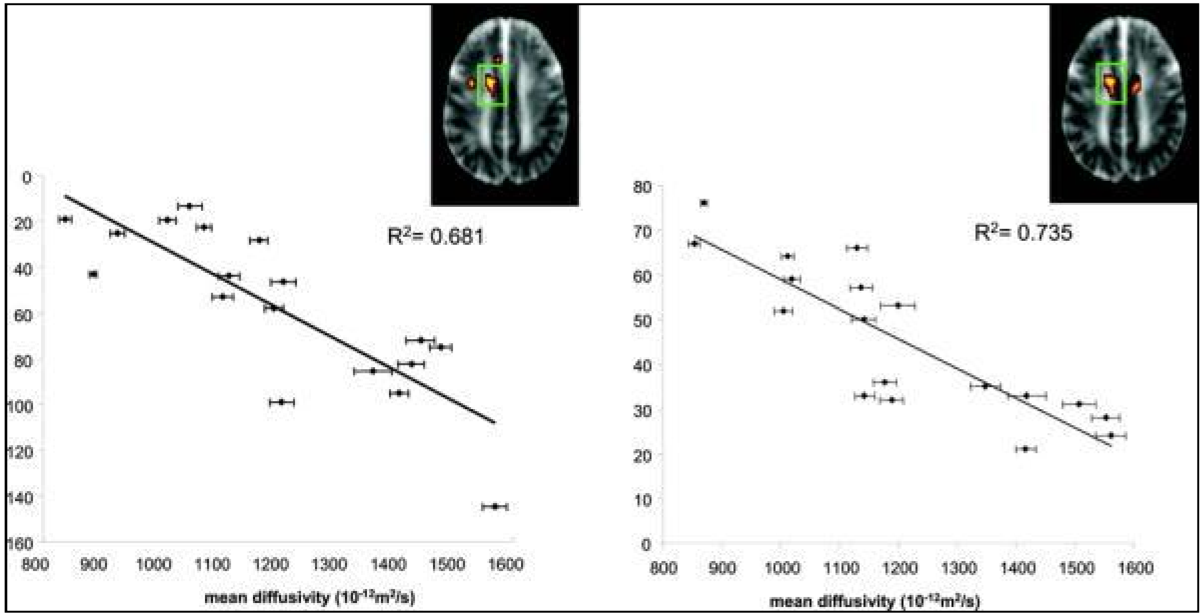

Figure 2 Cognitive set-shifting and the left cingulum bundle. On the scatter plots, each point represents an individual subject and plots mean diffusivity, averaged for the whole significant cluster, against performance. Insets show the clusters for each task. (Left) Trail Making B-A (s). (Right) Digit Symbol. Note that the values on the y axis have been reversed for Trail Making B-A to emphasize that performance declines as mean diffusivity in the cluster increases for both tasks (reflected as an increase in the time to complete Trail Making and a reduction in the number of correct responses for Digit Symbol).

Cross-Sectional DTI studies in MCI and AD

Study	year	Sample Size	Findings
Kantarci et al.	2010	30 DLB, 30 AD, 60 HC	diffusivity measures were complementary to structural measures, elevated diffusivity in DLB in amygdala with normal GM density (fundamental difference between AD and DLB)
Stricker et al.	2009	16 AD, 14 HC	late-myelinating fiber pathways show lower FA in AD than early-myelinating
Lee et al.	2009	47 AD, 73 MCI, 95 HC	Vascular and AD degenerative processes contribute to microstructural injury of cerebral WM
Fellgiebel et al.	2008	12 AD, 16 HC	cingulate bundles and IFOF are disturbed in AD; cingulate bundles important for verbal recognition
Nakata et al.	2008	23 AD, 18 HC	consistent with neuropathological data, posterior cingulate fiber tracts show decreased FA and increased MD; FA and MD reflect progression of AD-related histopathological changes in PCFT
Ukmar et al.	2008	14 AD, 15 MCI, 18 HC	FA decrease in MCI and AD in cc splenium; AD lower FA in cc genu right frontal WM; changes were associated with MMSE
Stahl et al.	2007	15 AD, 16 MCI, 19 HC	changes of ADC and FA values in AD and MCI; DTI is less applicable in detection of MCI than AD
Teipel et al.	2007	15 AD, 14 HC	dissociation between intracortical and extracortical projecting fibers systems in AD
Fellgiebel et al.	2005	17 aMCI, 25 AD, 21 HC	FA and MD changes of posterior cingulate bundle of MCI and AD patients; correlation of FA and MD with cognition

Summary of Cross-sectional Results

- Aging
  - relation between aging and white matter integrity - anterior-posterior gradient
  - relation between cognition and white matter integrity – consistent correlation with speed and executive functioning
- SVD
  - Areas of hyperintensity have different characteristcs on DTI
  - FA reduction and increase in MD in lesions and NAWM in both sporadic SVD and CADASIL
  - FA changes in NAWM correlate better with cognitive function than lesion load, peak height FA explains 74% of variance in executive functions if premorbid IQ is also considered
- MCI and AD
  - Focus on mean diffusivity (MD) and fractional anisotropy (FA) – alterations described in hippocampus, fornix, corpus callosum posterior cingulate/cingulum bundle, precuneus, medial and lateral temporal lobe, prefrontal lobe WM
  - Changes only partly independent of GM-atrophy
  - MD and FA in AD-related ROIs relate to cognitive impairment in demanding cognitive testing.
- New post-processing techniques offer additional opportunities

Diffusion Tensor Imaging

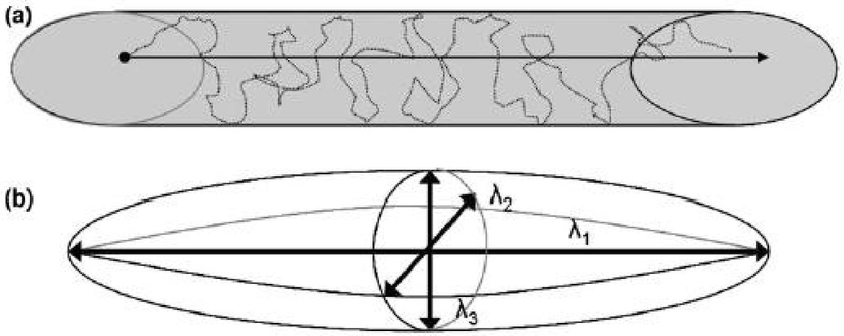

(c)

$$\hat{\lambda} = \begin{pmatrix} \lambda_1 & 0 & 0 \\ 0 & \lambda_2 & 0 \\ 0 & 0 & \lambda_3 \end{pmatrix}$$

Mean Diffusivity = $(\lambda_1+\lambda_2+\lambda_3)/3$

Fractional Anisotropy = $\sqrt{\frac{1}{2}} \frac{\sqrt{(\lambda_1-\lambda_2)^2+(\lambda_2-\lambda_3)^2+(\lambda_3-\lambda_1)^2}}{\sqrt{\lambda_1^2+\lambda_2^2+\lambda_3^2}}$

Axial (II) diffusivity = λ_1

Radial (T) diffusivity = $(\lambda_2+\lambda_3)/2$

MD = mean of all three axes of the diffusion ellipsoid and reflects the rate of water diffusion within a voxel, independently of the directionality.

FA= fraction of the tensor that can be assigned to anisotropic (directional) diffusion

Diffusion tensor imaging (DTI) probes mobility of water protons in the axons

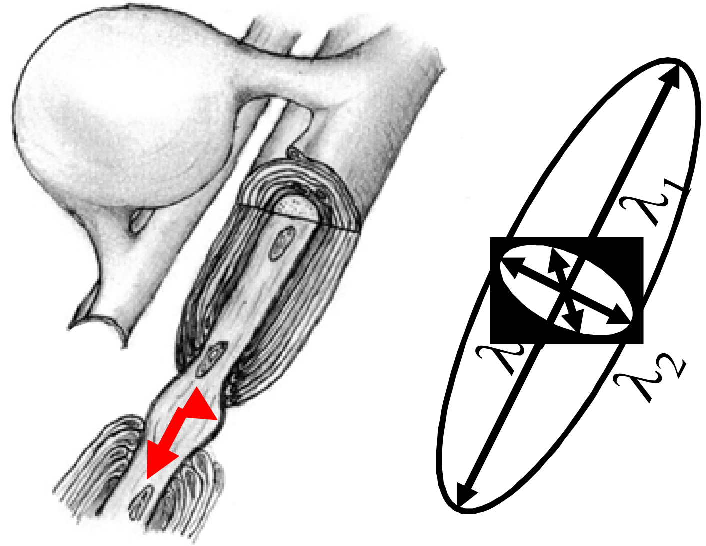

- restricted mobility in brain tissue
- modeled by a diffusion ellipsoid
- allows estimation of MD, FA, RD, AD

ELSEVIER

NeuroImage

www.elsevier.com/locate/ynimg
NeuroImage 40 (2008) 1–10

Evolving Wallerian degeneration after transient retinal mice characterized by diffusion tensor imaging

Shu-Wei Sun,[a] Hsiao-Fang Liang,[a] Anne H. Cross,[b] and Sheng-Kwei Song[a,*]

[a]Department of Radiology, Washington University School of Medicine, St. Louis, MO, USA
[b]Department of Neurology, Washington University School of Medicine, St. Louis, MO, USA

Received 9 April 2007; revised 26 November 2007; accepted 28 November 2007
Available online 8 December 2007

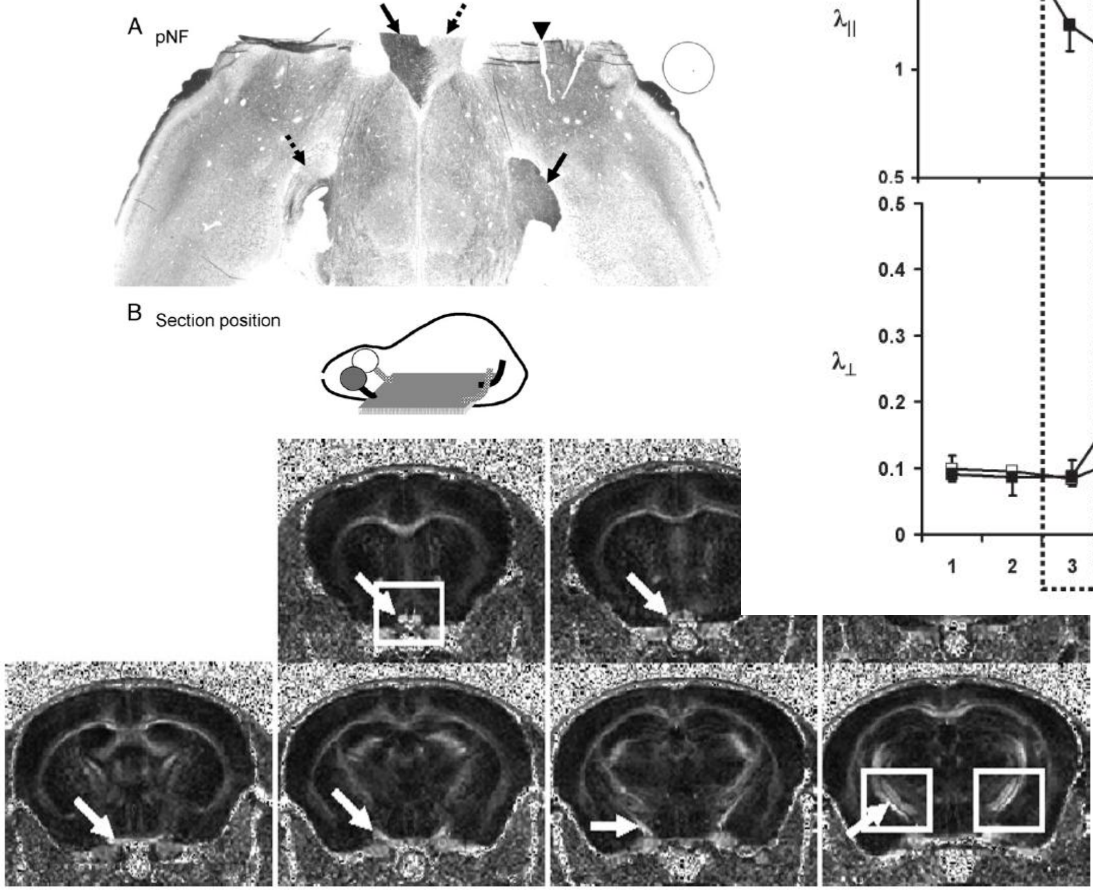

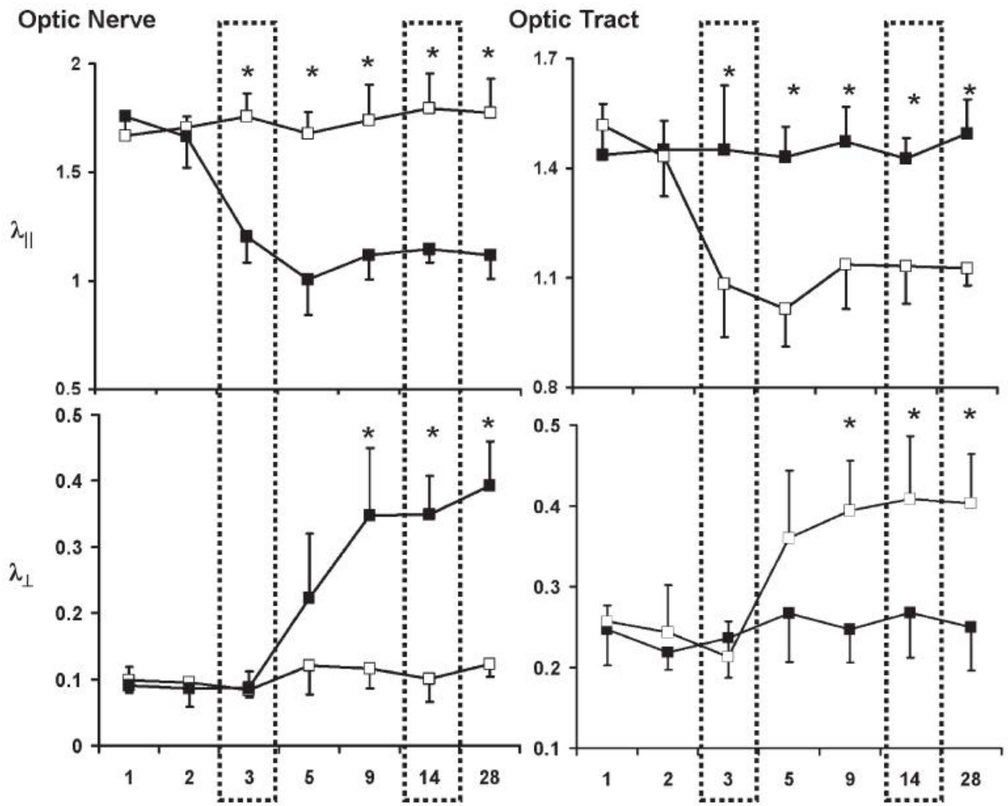

The JAMA Network

From: **White Matter Microstructural Integrity and Cognitive Function in a General Elderly Population**

Arch Gen Psychiatry. 2009;66(5):545-553. doi:10.1001/archgenpsychiatry.2009.5

Table 4. Linear Regression Models for DTI Parameters in Normal-Appearing White Matter in Relation to Cognitive Function[a]

	Mean Change in *z* Score per Standard Deviation Increase (95% Confidence Interval)				
	Memory	Executive Function	Information Processing Speed	Global Cognition	Motor Speed
Age[b]	−0.02 (−0.04 to −0.01)[c]	−0.05 (−0.06 to −0.04)[c]	−0.04 (−0.05 to −0.03)[c]	−0.04 (−0.05 to −0.03)[c]	−0.05 (−0.06 to −0.04)[c]
Normal-appearing white matter volume[b,d]	0.01 (−0.07 to 0.07)	0.14 (0.09 to 0.20)[c]	0.15 (0.09 to 0.21)[c]	0.10 (0.05 to 0.15)[c]	0.09 (0.02 to 0.16)[c]
Mean MD in normal-appearing white matter					
Model 1	−0.02 (−0.09 to 0.05)	−0.11 (−0.16 to −0.05)[c]	−0.12 (−0.18 to −0.07)[c]	−0.08 (−0.13 to −0.03)[c]	−0.10 (−0.17 to −0.02)[c]
Model 2	−0.02 (−0.10 to 0.05)	−0.08 (−0.14 to −0.03)[c]	−0.10 (−0.16 to −0.04)[c]	−0.06 (−0.11 to −0.01)[c]	−0.08 (−0.16 to −0.01)[c]
Model 3	−0.01 (−0.08 to 0.07)	−0.10 (−0.16 to −0.04)[c]	−0.13 (−0.19 to −0.07)[c]	−0.07 (−0.12 to −0.02)[c]	−0.08 (−0.16 to 0.00)[c]
Model 4	−0.01 (−0.09 to 0.07)	−0.07 (−0.13 to −0.02)[c]	−0.11 (−0.17 to −0.05)[c]	−0.05 (−0.11 to 0.00)[c]	−0.06 (−0.14 to 0.01)
Model 5	0.01 (−0.07 to 0.09)	−0.07 (−0.13 to −0.01)[c]	−0.10 (−0.17 to −0.04)[c]	−0.05 (−0.11 to 0.00)[c]	−0.04 (−0.12 to 0.04)
Model 6	−0.01 (−0.08 to 0.07)	−0.07 (−0.13 to −0.02)[c]	−0.11 (−0.17 to −0.04)[c]	−0.05 (−0.10 to 0.00)[c]	−0.06 (−0.14 to 0.01)
Mean FA in normal-appearing white matter					
Model 1	−0.02 (−0.09 to 0.05)	0.04 (−0.01 to 0.10)	0.06 (0.00 to 0.12)[c]	0.03 (−0.02 to 0.07)	0.07 (0.01 to 0.14)[c]
Model 2	−0.02 (−0.09 to 0.05)	0.04 (−0.01 to 0.09)	0.06 (0.00 to 0.11)[c]	0.02 (−0.02 to 0.07)	0.08 (0.01 to 0.14)[c]
Model 3	−0.03 (−0.10 to 0.04)	0.03 (−0.02 to 0.09)	0.06 (0.00 to 0.12)[c]	0.02 (−0.03 to 0.07)	0.06 (−0.01 to 0.13)
Model 4	−0.03 (−0.10 to 0.04)	0.03 (−0.02 to 0.09)	0.06 (0.01 to 0.12)[c]	0.02 (−0.03 to 0.06)	0.06 (−0.01 to 0.13)
Model 5	−0.04 (−0.11 to 0.03)	0.03 (−0.03 to 0.08)	0.05 (−0.01 to 0.11)	0.01 (−0.04 to 0.06)	0.05 (−0.02 to 0.12)
Model 6	−0.03 (−0.10 to 0.04)	0.04 (−0.01 to 0.09)	0.07 (0.01 to 0.12)[c]	0.02 (−0.03 to 0.07)	0.06 (−0.01 to 0.13)
Mean λ_{ax} in normal-appearing white matter					
Model 1	−0.04 (−0.11 to 0.03)	−0.11 (−0.17 to −0.06)[c]	−0.13 (−0.19 to −0.07)[c]	−0.08 (−0.14 to −0.04)[c]	−0.09 (−0.16 to −0.02)[c]
Model 2	−0.04 (−0.11 to 0.03)	−0.08 (−0.14 to −0.03)[c]	−0.10 (−0.16 to −0.04)[c]	−0.07 (−0.12 to −0.02)[c]	−0.07 (−0.14 to 0.00)[c]
Model 3	−0.03 (−0.10 to 0.05)	−0.10 (−0.16 to −0.05)[c]	−0.14 (−0.20 to −0.08)[c]	−0.08 (−0.13 to −0.03)[c]	−0.07 (−0.15 to 0.00)[c]
Model 4	−0.03 (−0.11 to 0.05)	−0.07 (−0.13 to −0.02)[c]	−0.11 (−0.17 to −0.04)[c]	−0.06 (−0.11 to −0.01)[c]	−0.05 (−0.13 to 0.02)
Model 5	−0.01 (−0.09 to 0.06)	−0.07 (−0.13 to −0.02)[c]	−0.11 (−0.17 to −0.04)[c]	−0.06 (−0.11 to 0.00)[c]	−0.03 (−0.11 to 0.05)
Model 6	−0.03 (−0.10 to 0.05)	−0.07 (−0.13 to −0.02)[c]	−0.10 (−0.17 to −0.04)[c]	−0.06 (−0.11 to −0.01)[c]	−0.06 (−0.13 to 0.02)
Mean λ_{rad} in normal-appearing white matter					
Model 1	0.01 (−0.08 to 0.06)	−0.10 (−0.16 to −0.05)[c]	−0.12 (−0.18 to −0.06)[c]	−0.07 (−0.12 to −0.02)[c]	−0.10 (−0.17 to −0.02)[c]
Model 2	0.01 (−0.08 to 0.06)	−0.08 (−0.13 to −0.02)[c]	−0.09 (−0.15 to −0.04)[c]	−0.05 (−0.10 to −0.01)[c]	−0.08 (−0.16 to −0.01)[c]
Model 3	0.00 (−0.07 to 0.08)	−0.09 (−0.15 to −0.04)[c]	−0.13 (−0.19 to −0.07)[c]	−0.06 (−0.11 to −0.01)[c]	−0.08 (−0.15 to 0.00)[c]
Model 4	0.00 (−0.07 to 0.08)	−0.07 (−0.13 to −0.01)[c]	−0.10 (−0.17 to −0.04)[c]	−0.05 (−0.10 to 0.00)	−0.06 (−0.14 to 0.01)
Model 5	0.02 (−0.06 to 0.10)	−0.06 (−0.12 to −0.01)[c]	−0.10 (−0.16 to −0.04)[c]	−0.04 (−0.09 to 0.01)	−0.05 (−0.12 to 0.03)
Model 6	0.01 (−0.07 to 0.08)	−0.07 (−0.13 to −0.01)[c]	−0.10 (−0.17 to −0.04)[c]	−0.05 (−0.10 to 0.00)	−0.06 (−0.14 to 0.01)

Abbreviations: DTI, diffusion tensor imaging; FA, fractional anisotropy; MD, mean diffusivity; λ_{ax}, axial diffusivity; λ_{rad}, radial diffusivity.

[a] Model 1: adjusted for age, sex, and level of education. Model 2: same as model 1, additionally adjusted for normal-appearing white matter volume.[d] Model 3: same as model 1, additionally adjusted for white matter lesion volume.[d,e] Model 4: same as model 1, additionally adjusted for both normal-appearing white matter volume[d] and white matter lesion volume.[d,e] Model 5: same as model 4, additionally adjusted for systolic blood pressure, diastolic blood pressure, serum total cholesterol level, diabetes mellitus, smoking status, use of blood pressure–lowering drugs, and use of lipid-lowering drugs. Model 6: same as model 4, additionally adjusted for relative temporal lobe volume.

[b] Adjusted for age (if applicable), sex, and level of education.

[c] Significant at $P < .05$.

[d] Expressed as percentage of intracranial volume.

[e] Natural log transformed.

Different Patterns of White Matter Degeneration Using Multiple Diffusion Indices and Volumetric Data in Mild Cognitive Impairment and Alzheimer Patients

Gilberto Sousa Alves[1,4*], Laurence O'Dwyer[4], Alina Jurcoane[6], Viola Oertel-Knöchel[4], Christian Knöchel[4], David Prvulovic[4], Felipe Sudo[1], Carlos Eduardo Alves[1], Letice Valente[1], Denise Moreira[3,5], Fabian Fußer[4], Tarik Karakaya[4], Johannes Pantel[6], Eliasz Engelhardt[1,2], Jerson Laks[1]

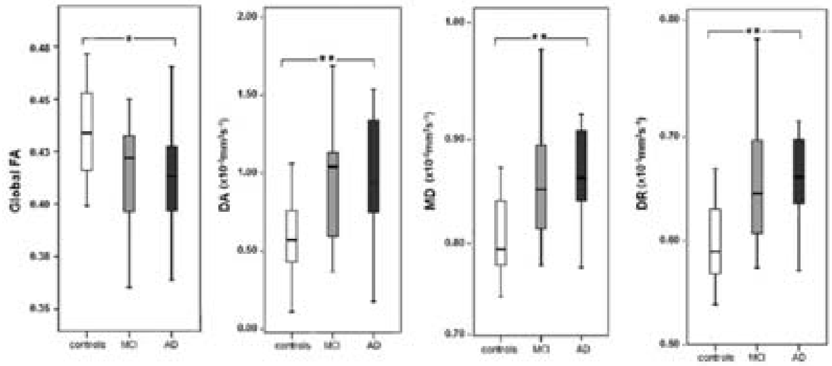

Figure 1. Distribution of diffusion tensor MRI indices for the global WM ROI in controls, MCI and AD patients. Multivariate Analysis reported significant differences between groups for FA ($F = 4.649$, $df = 2$, $P<0.05$), axial diffusivity ($F = 5.610$, $df = 2$, $P<0.05$), MD ($F = 6.821$, $df = 2$, $P<0.005$) and radial diffusivity ($F = 7.131$, $df = 2$, $P<0.005$). $^*P<0.05$, $^{**}P<0.01$, corrected for multiple comparisons using Bonferroni correction.

Figure 2. TBSS maps showing voxelwise comparisons between patients and controls. The mean FA skeleton (green voxels) projected on the FMRIB template brain. Low FA in AD patients in is shown in dark red (A); low FA in MCI is shown in yellow-red (B); high MD in AD is depicted in blue (C) and high radial diffusivity in orange.

doi:10.1371/journal.pone.0052859.g002

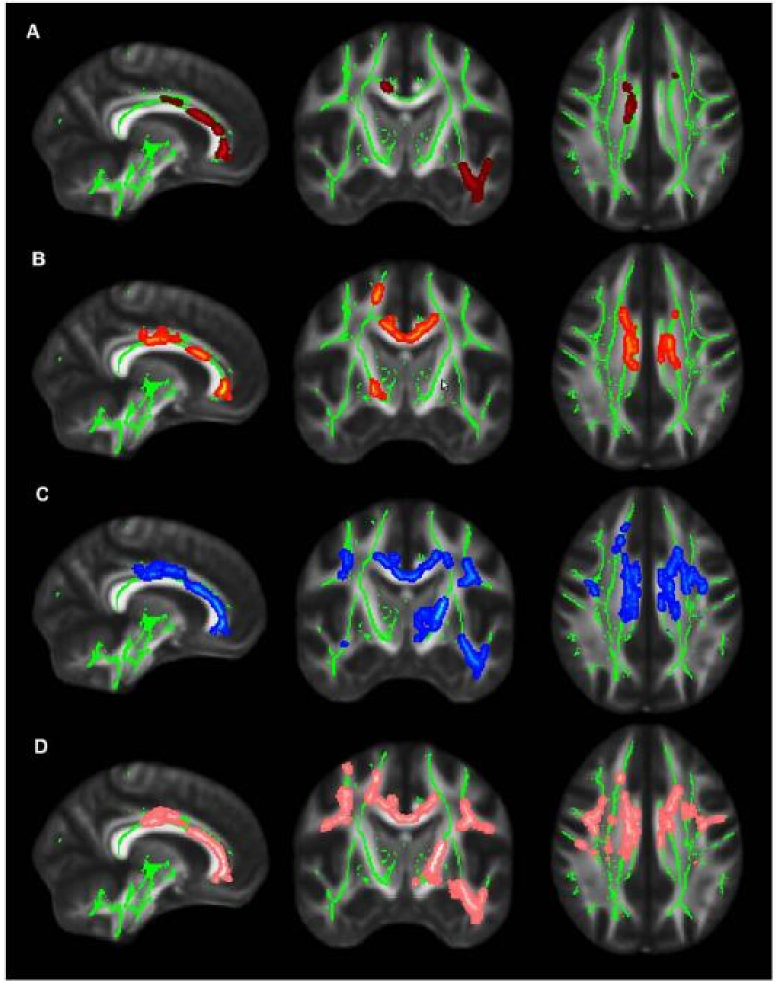

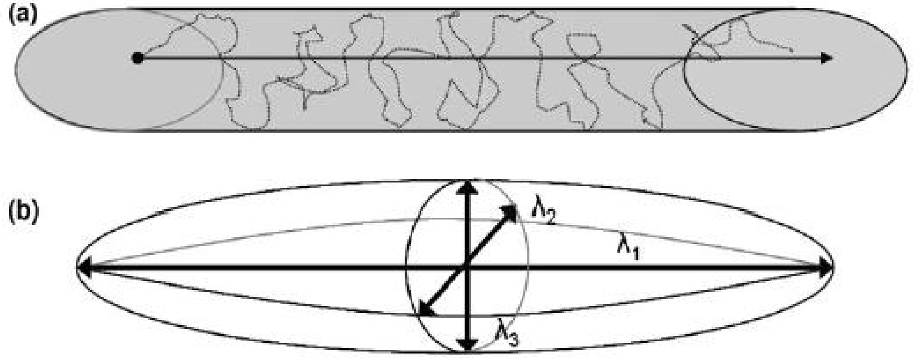

(c)

$$\hat{\lambda} = \begin{pmatrix} \lambda_1 & 0 & 0 \\ 0 & \lambda_2 & 0 \\ 0 & 0 & \lambda_3 \end{pmatrix}$$

Mean Diffusivity = $(\lambda_1+\lambda_2+\lambda_3)/3$

Fractional Anisotropy = $\sqrt{\frac{1}{2}}\frac{\sqrt{(\lambda_1-\lambda_2)^2+(\lambda_2-\lambda_3)^2+(\lambda_3-\lambda_1)^2}}{\sqrt{\lambda_1^2+\lambda_2^2+\lambda_3^2}}$

Axial (II) diffusivity = λ_1

Radial (T) diffusivity = $(\lambda_2+\lambda_3)/2$

Longitudinal DTI studies in normal aging and SVD

Study	Subjects	Cognitive measures	Conclusion
Charlton et al	84 Healthy volunteers	NART, trails, D-KEFS, towers, letter fluency, category fluency, Stoop, WICST, digit span backwards, letter number sequencing, AMIPB, WAISR, grooved peg-board	Median MD increased and FA decreased over two-years. MD changes correlated with change in working memory
Jokinen et al	340 LADIS participants	MMSE, VADAS, Stroop, trails	DWI microstructural changes in NABT predict faster decline in psychomotor speed, executive functions, and working memory regardless of conventional MRI findings. Moreover, these changes are related to functional disability and higher mortality.
Nitkunan et al	27 lacunar infarcts and SVD	NART, MMSE, MDRS, trails, verbal fluency, digit span, WAIS, delayed recall	FA correlated with executive function and Rankin. MD correlated with global cognitive score. After one-year, significant increase in median MD and nonsignificant decrease in median FA. No change in cognitive scores
Holtmannspotter et al	62 CADASIL	Modified Rankin, Barthel, NIHSS, SIDAM, MDRS	MD significantly increased in two-years. Change in MD correlated with deterioration in Rankin, NIHSS and SIDAM

Diffusion Changes Predict Cognitive and Functional Outcome: The LADIS Study

Hanna Jokinen, PhD,[1,2] Reinhold Schmidt, MD,[3] Stefan Ropele, PhD,[3]
Franz Fazekas, MD,[3] Alida A. Gouw, MD, PhD,[4] Frederik Barkhof, MD, PhD,[4]
Philip Scheltens, MD, PhD,[4] Sofia Madureira, PsyD,[5] Ana Verdelho, MD,[5]
José M. Ferro, MD, PhD,[5] Anders Wallin, MD, PhD,[6] Anna Poggesi, MD, PhD,[7]
Domenico Inzitari, MD,[7] Leonardo Pantoni, MD, PhD,[7]
and Timo Erkinjuntti, MD,[1] on behalf of the LADIS Study Group

TABLE 2: Association of the ADC Histogram Metrics with the Rate of Cognitive Decline during 3-Year Follow-up (4 Assessments at Yearly Intervals)[a]

Metric	MMSE	VADAS	Speed	Executive	Memory
NABT mean global ADC					
Model I	1.5 (0.226)	0.6 (0.596)	7.6 (<0.001)	2.0 (0.119)	5.4 (0.001)
Model II	1.3 (0.273)	0.6 (0.599)	7.9 (<0.001)	1.7 (0.161)	5.2 (0.002)
Model III	0.7 (0.539)	0.4 (0.788)	5.9 (<0.001)	2.9 (0.036)	3.0 (0.030)
NABT peak height					
Model I	3.0 (0.032)	2.7 (0.047)	8.2 (<0.001)	3.2 (0.024)	4.9 (0.003)
Model II	2.9 (0.038)	2.6 (0.054)	8.2 (<0.001)	3.1 (0.026)	5.5 (0.001)
Model III	1.6 (0.197)	1.6 (0.189)	8.7 (<0.001)	5.5 (0.001)	4.3 (0.006)
NABT peak position					
Model I	1.5 (0.221)	0.3 (0.858)	5.7 (<0.001)	1.6 (0.181)	0.9 (0.434)
Model II	1.5 (0.225)	0.2 (0.881)	5.9 (<0.001)	1.4 (0.231)	0.8 (0.482)
Model III	1.6 (0.197)	0.4 (0.725)	5.0 (0.002)	1.9 (0.136)	0.2 (0.909)
WMH mean ADC					
Model I	0.8 (0.477)	0.8 (0.471)	5.9 (<0.001)	1.4 (0.244)	2.8 (0.038)
Model II	0.8 (0.498)	0.9 (0.455)	6.0 (<0.001)	1.3 (0.275)	2.8 (0.041)
Model III	0.8 (0.472)	0.7 (0.576)	2.9 (0.035)	0.3 (0.807)	1.7 (0.172)

[a]Linear mixed models, diffusion-weighted imaging predictor × time interactions given as F (p value). Model I = adjusted for age, gender, and education (total n = 340). Model II = additional adjustment for WMH volume and lacunes (available for 334 subjects). Model III: additional adjustment for global brain atrophy (available for 257 subjects).ADC = apparent diffusion coefficient; MMSE = Mini-Mental State Examination; NABT = normal-appearing brain tissue; VADAS = Vascular Dementia Assessment Scale; WMH = white matter hyperintensities.

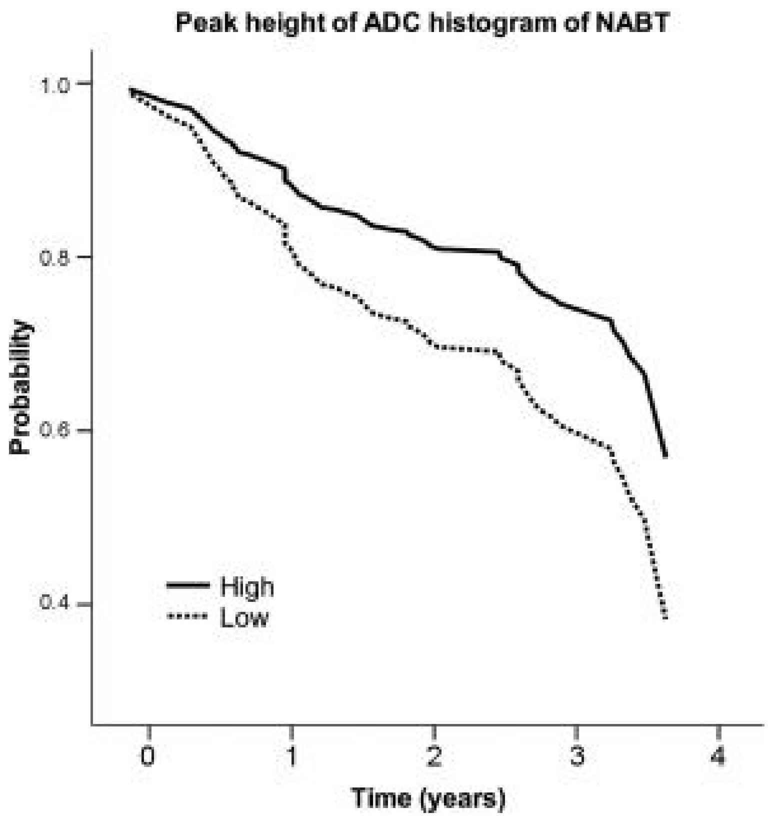

Annals of Neurology
Volume 73, Issue 5, pages 576-583, 19 FEB 2013 DOI: 10.1002/ana.23802
http://onlinelibrary.wiley.com/doi/10.1002/ana.23802/full#ana23802-fig-0001

Longitudinal DTI studies in MCI and AD

Study	FU-period	Subjects	Mean age	Measures	Cognitive measures	Conclusion
Haller et al. Journal of Alzheimer's Disease. 2010, 22(1), 315-327	DTI baseline - 1 year neuropsy. FU	35 HC, 67 MCI (40 stable MCI, 27 progressive MCI)	n.A.	FA, MD, l ,[illegible]	n.A.	SVM analyses of DTI data provide high accurate individual classification of stable vs. progressive MCI: it might become an easy applicable tool for early individual detection of MCI subjects evolving to dementia
Likitjaroen et al. Eur Arch Psychiatry Clin Neurosci. 2012, 262, 341-350.	1 year	11 HC 28 AD (Galantamine + placebo group)	67.4 ± 7.7 73.5 ± 7.2 76.4 ± 7.9	FA	MMSE, CERAD, CDR	DTI demonstrated FA decline in intracortically projecting fibre tracts in aging and AD; galantamine had limited impact in regional FA decline
Mielke et al. Alzheimer's & Dementia. 2012, 8, 105-113.	1 and 2.5 years, resp.	23 MCI (6 converted to AD, 17 remained stable during FU period)	75.6 ± 5.5 78.7 ± 2.9 74.5 ± 5.8	FA, MD, l ,[illegible]	MMSE, CDR, ADAS-cog, CVLT, Log. Memory A of WMS, TMT A and COWAT	Fornix FA correlated with and longitudinally predicted memory decline and progression to AD;
Nowrangi et al. Alzheimer's & Dementia. 2012, 1-10.	1 year	25 HC 25 aMCI 25 AD	74.3 ± 7.1 75.8 ± 5.3 75.6 ± 7.0	FA, MD	n.A.	over FU-period MD was a better predictor of change than FA; increases of MD in the fornix in MCI suggest this as an early indicator of progression
Selnes et al. Journal of Alzheimer's Disease. 2013, 33, 723-736.	2-3 years	21 HC 11 SCI 43 MCI	64.3 (53-75) 61.3 (52-71) 62.1 (50-77)	FA, MD, l?á, Ab42, T-tau, P-tau	MMSE, GDS, Cognisat, CDR, STEP, I-Flex	DTI surpasses CSF as predictor of cognitive decline

Summary of Longitudinal Results

- FA and MD changes parallel cognitive deterioration
- In MCI and AD FA decrease is in the range of percent volume loss of hippocampal volume over time (up to 7%/per year). Fiber tract changes have strong temporal dynamics above the age of 60
- DTI measures predict not only cognitive decline but also disability and death, and may be useful to distinguish between stable and progressive MCI
- Very limited data on the use for monitoring treatment effects

Change of average MD versus the change of clinical status during follow-up in the 62 CADASIL subjects: (A) disability scores (Rankin); (B) cognitive scores (SIDAM).

Variable	No. of Subjects Needed to Include	
	Minimum Treatment Effect=20%	Minimum Treatment Effect=40%
T2-lesion volumes, whole brain	1532	384
T2-lesion volumes, central slices	3822	958
Average mean diffusivity	1944	488
Stroke occurrence	2732	620
Rankin scale scores	7452	1864
SIDAM scores	7662	1918

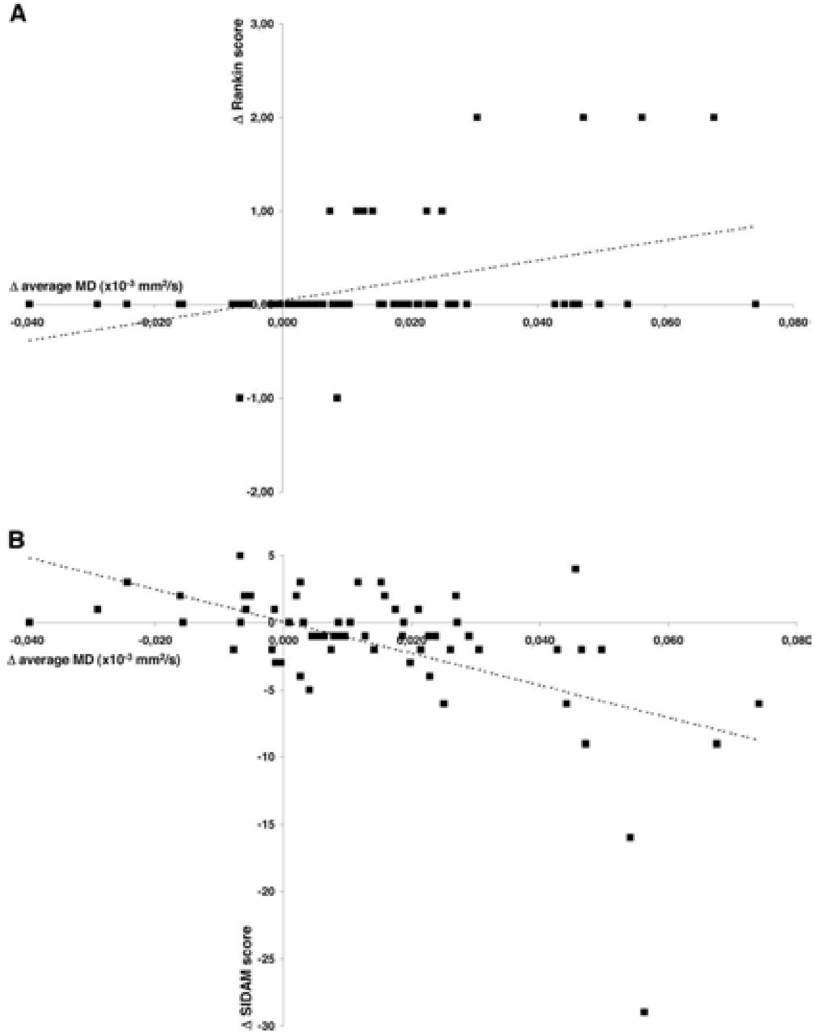

Holtmannspötter M et al. Stroke 2005;36:2559-2565

The influence of treatment on microstrucutre

Longitudinal changes of fractional anisotropy in Alzheimer's disease patients treated with galantamine: a 12-month randomized, placebo-controlled, double-blinded study

Y. Likitjaroen · T. Meindl · U. Friese · M. Wagner · K. Buerger · H. Hampel · S. J. Teipel

- 28 AD patients, 11 healthy controls
- 6 month double blind galantamine treatment vs. placebo
- 6 month open label extension phase
- DTI at BL, 6 and 12 months
- FA in ROIs

- Results:
  - Differences in age, years of education, MMSE and all CERAD subtests between AD and HC (AD older, less educated, worse cognitive performance)
  - No within-group differences in age, years of education, MMSE and all CERAD subtests in AD (treated vs. placebo)

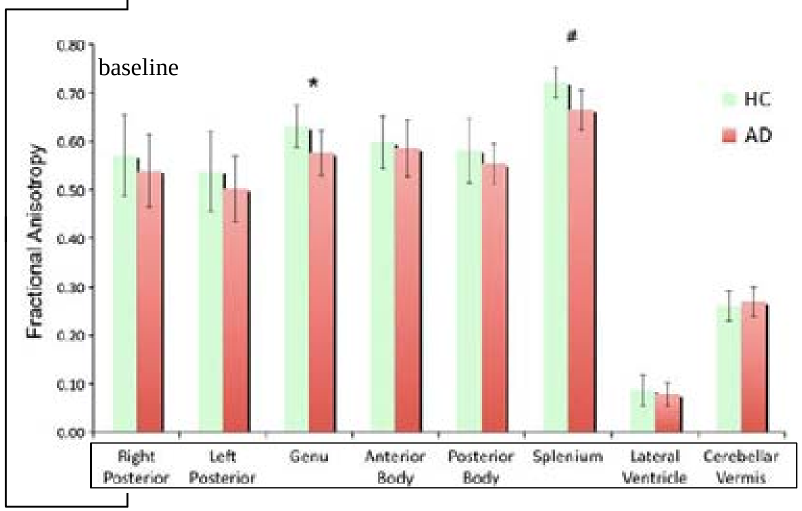

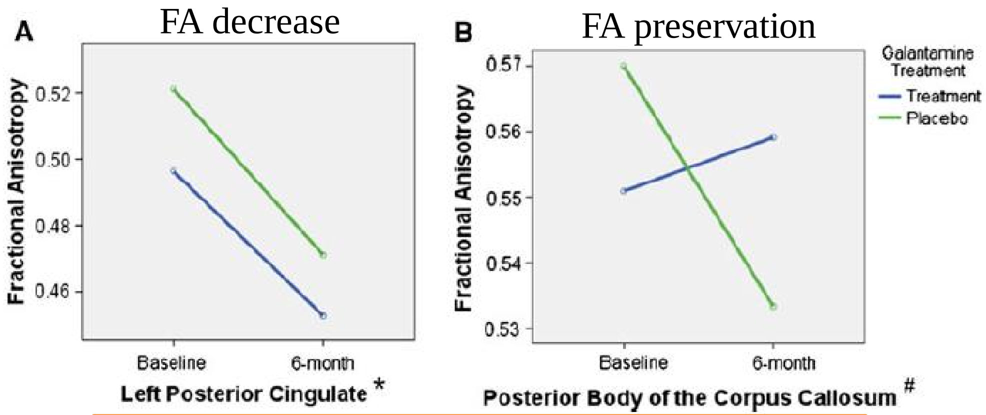

No other region showed significant differences in FA comparing treatment and placebo group

Magnetization Transfer Imaging

The focus is rather on tissue composition than on tissue organization. It´s role in comparision to DTI is widely unexplored

Magnetization transfer (MT) imaging probes magnetization exchange between tissue water and protons bound to macromolecules (myelin)

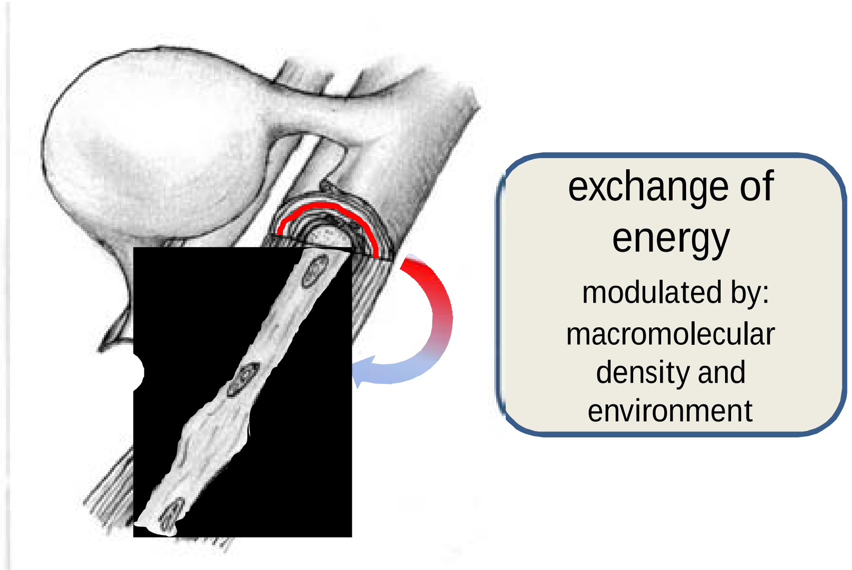

- assessed by the magnetization transfer ratio (MTR) or
- true quantitatively by qMT

Quantifying the effect of MT:
The magnetization transfer ratio (MTR)

$$MTR = \left(\frac{S_0 - S_S}{S_0} \right) \times 100\%$$

S_0 …. reference scan
S_S …. MT weighted scan

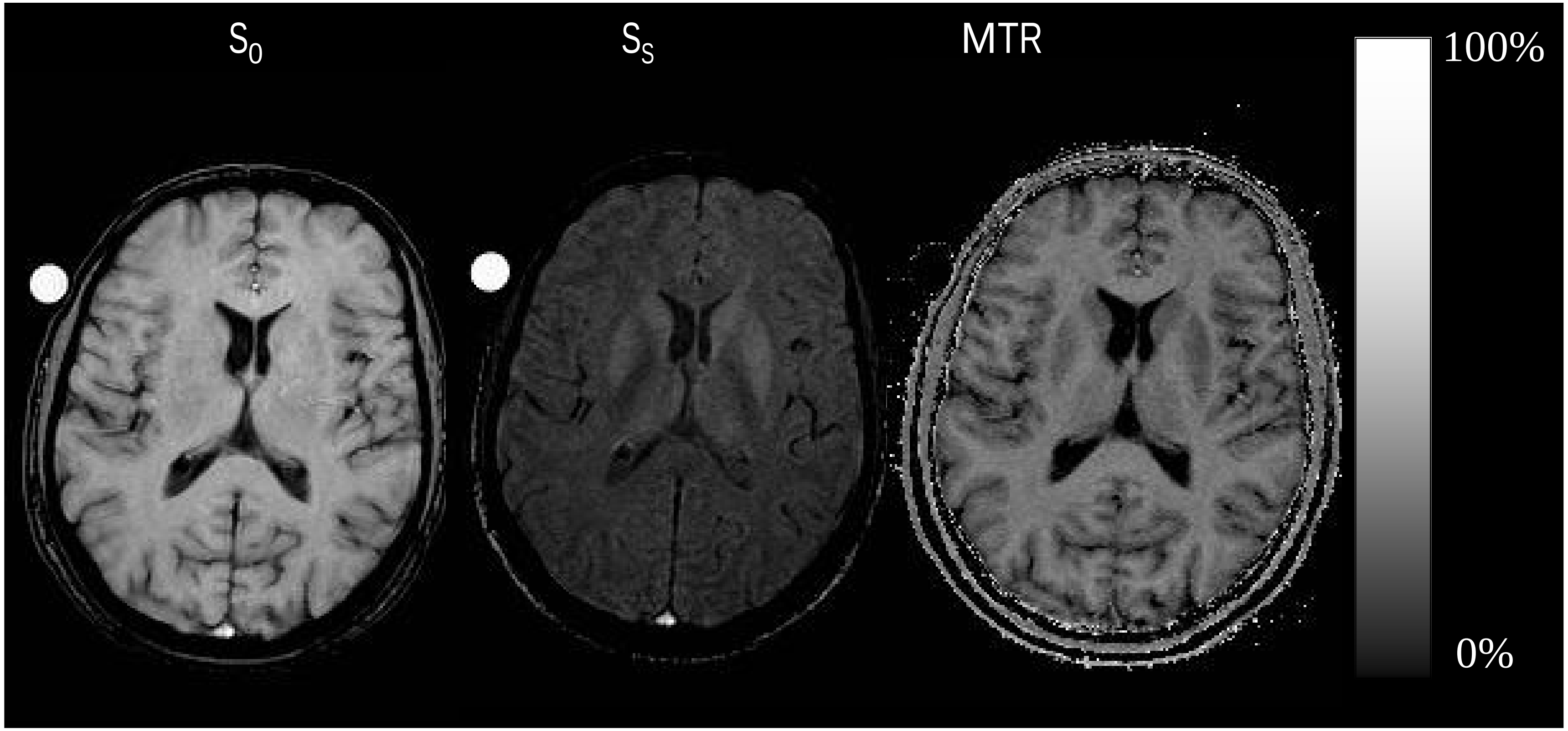

Histopathologic Correlations MTR

	r	*p*
MTR vs TR_{myelin}	-0.84	<0.001
MTR vs Axonal count	0.66	<0.001
TR_{myelin} vs Axonal count	-0.80	<0.001
MTR vs $TR_{gliosis}$	0.13	0.370

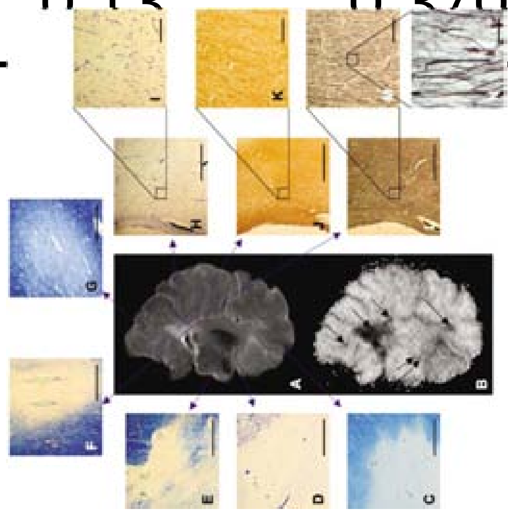

Klaus Schmierer et al.
Ann Neurol 2004;56:407.

MTI in normal ageing

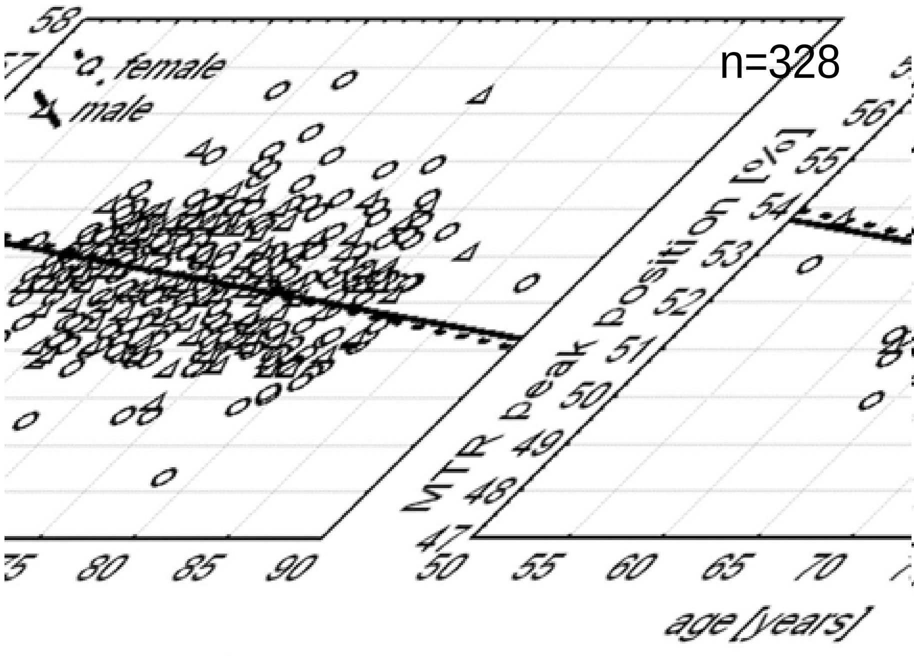

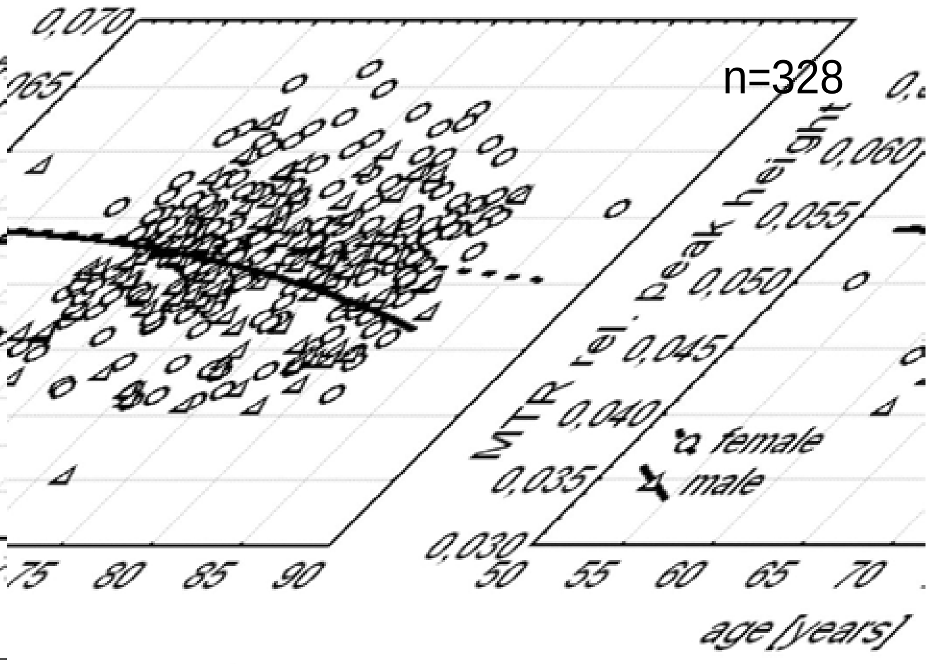

The impact of sex and vascular risk factors on brain tissue changes with ageing.

Ropele S, Enzinger C, Söllinger M, Langkammer C, Wallner-Blazek M, Schmidt R, Fazekas F.
AJNR Am J Neuroradiol. 2010

- § Microstructural changes increase with ageing
- § More extensive in men
- § Diabetes and hypertension add to tissue destruction

Cross-sectional results of MTI studies in normal aging, SVD and Alzheimer´s Disease

Study	Year	Sample Size	Findings
Fazekas	2005 Brain	198 ASPS participants	Non-significant trend for association between motor skills and frontal NAWM MTR
Schiavone	2009 J Magn Res Imaging	106 elderly adults	All MRI parameters correlated with cognition, but DTI, and particularly FA, correlated most strongly. Adding DTI parameters explained more variance in cognition than WMH alone; the increase was greatest with FA, which alone explained 45%, 33%, and 25% of the variance in cognition for information processing speed, episodic memory, and executive function, respectively.
Hanyu	2005 Neurosci Lett	DLB/17 AD/31 C/18	Hippocampal MTR sensitivity of 76% and specificity of 71% to discriminate DLB from AD.
Van Es	2006 Neurobiol Aging	AD/55 MCI/19 C/43	MTI changes that are related to cognitive impairment in both GM and WM of patients with AD and MCI.
Ridha	2007 AJNR	AD/18 C/18	Hc mean MTR added no statistically significant discriminatory value over and above Hc volume measurement alone. WB volume was significantly correlated with MMSE
Ridha	2007 Radiology	AD/14 C/14	Certain MT parameters may serve as useful biomarkers of AD.
Kiefer	2009 Neuroimage	AD/12 MCI/10 C/22	qMT-parameters (T2 of the restricted pool) and F (fractional pool size) differentiated between C, MCI and AD in the anterior hippocampus
Fornari	2012 Neurobiol Aging	Early AD/15 C/15	Different patterns of superficial WM demyelination. SWMD impacts cognition

JOURNAL OF MAGNETIC RESONANCE IMAGING 29:23–30 (2009)

Original Research

Imaging Age-Related Cognitive Decline: A Comparison of Diffusion Tensor and Magnetization Transfer MRI

Francesca Schiavone, MSc,[1*] Rebecca Ann Charlton, PhD,[1] Thomas Richard Barrick, PhD,[1]
Robin Guy Morris, PhD,[2] and Hugh Stephen Markus, DM, FRCP[1]

Correlation Between MRI Parameters and Cognitive Domains

	MRI		
	MD	FA	MT
Information processing speed	r = 0.606 *P* <0.0001	r = 0.668 *P* < 0.0001	r = 0.486 *P* <0.0001
Working memory	r = 0.334 *P* < 0.007	r = 0.286 *P* = 0.022	r = 0.113 *P* = 0.375
Executive function	r = 0.454 *P* < 0.0001	r = 0.503 *P* < 0.001	r = 0.412 *P* < 0.001
Episodic memory	r = 0.398 *P* < 0.001	r = 0.574 *P* < 0.0005	r = 0.376 *P* < 0.003

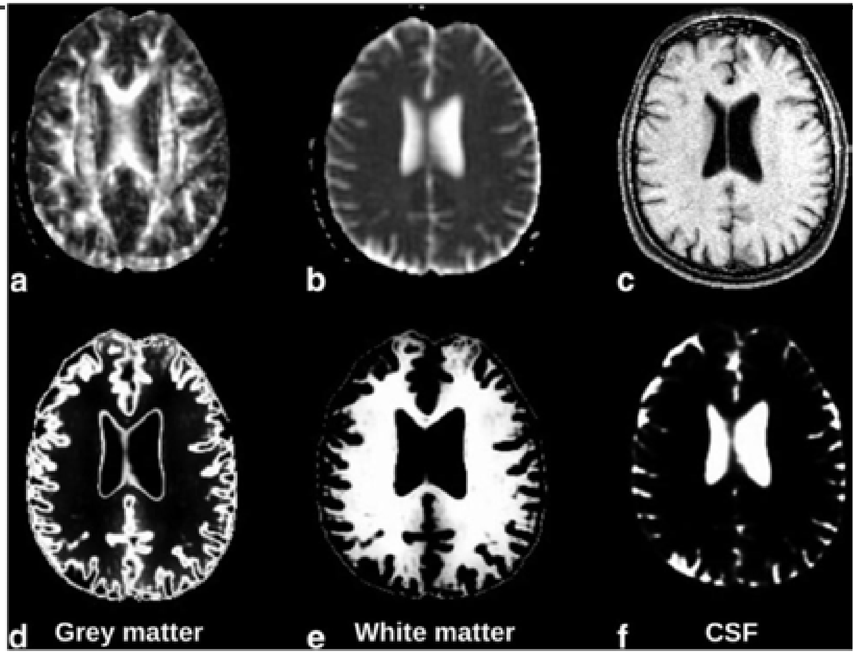

Severity of tissue changes measured by magnetization transfer imaging

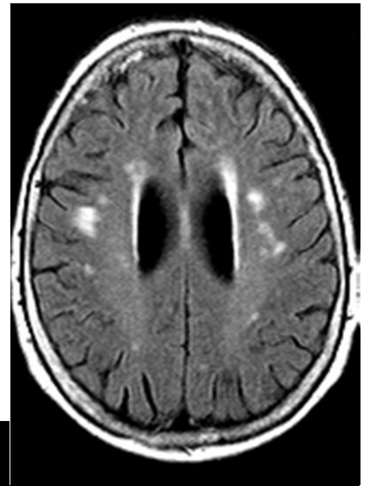

- 198 volunteers (136 female, 62 male)
- Age range: 52 to 87 years (mean age 70 years)
- Normal appearing white matter, grey matter and WMH

Fazekas F. et al. Brain 2005; 128:2926-2932

MESCOG
funded by ERA-NET NEURON

A: Neocortex whole brain

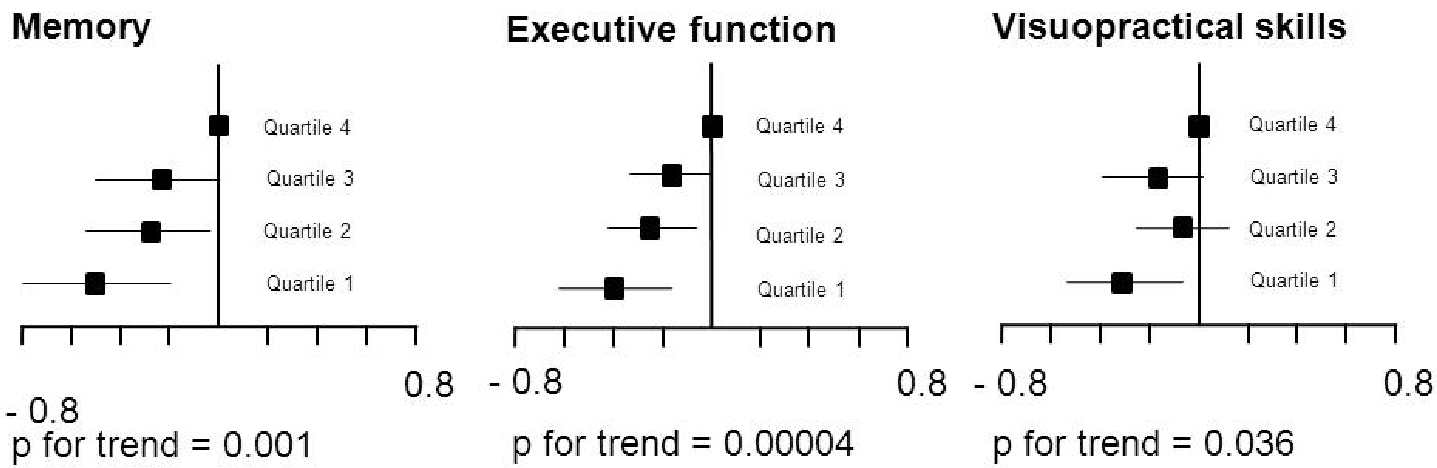

B: NAWM whole brain

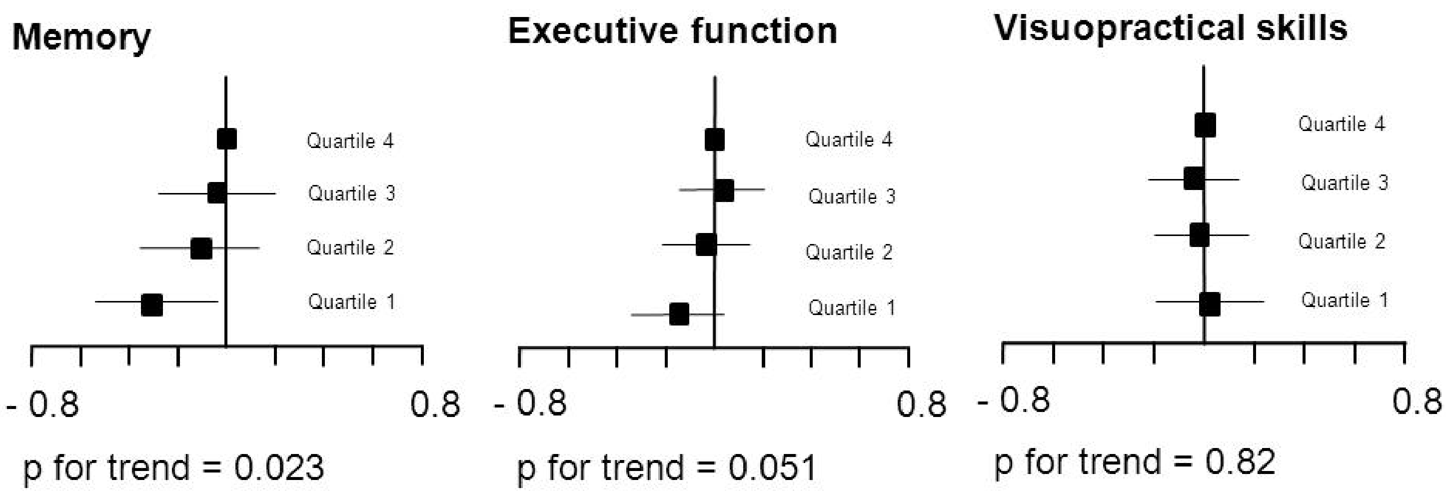

Contents lists available at SciVerse ScienceDirect

NeuroImage

journal homepage: www.elsevier.com/locate/ynimg

Quantitative magnetization transfer provides information complementary to grey matter atrophy in Alzheimer's disease brains

Giovanni Giulietti [a,*], Marco Bozzali [a], Viviana Figura [a], Barbara Spanò [a], Roberta Perri [b], Camillo Marra [c], Giordano Lacidogna [c], Franco Giubilei [d], Carlo Caltagirone [b,e], Mara Cercignani [a]

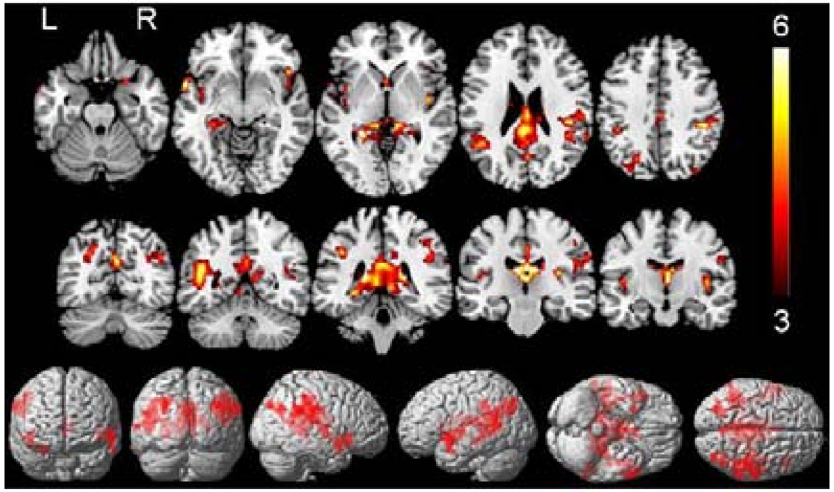

Voxel-wise analysis

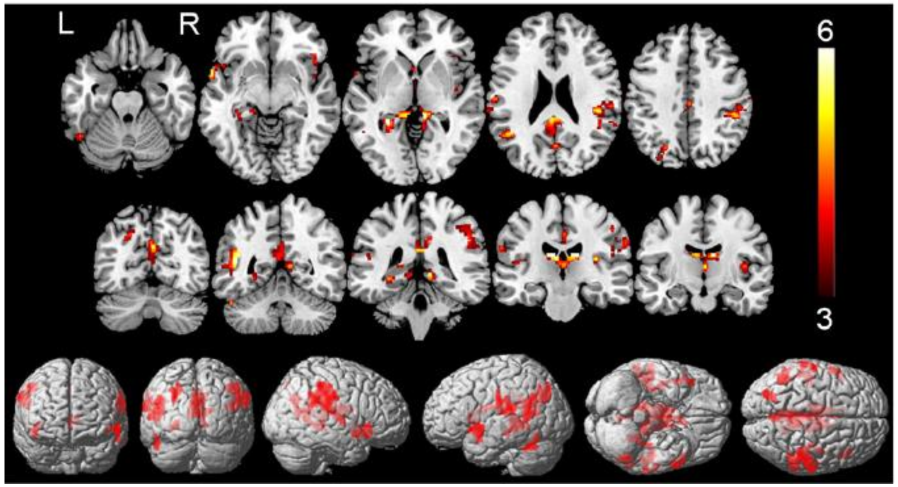

Multimodal analysis adjusting for grey matter volume

Longitudinal Magnetization Transfer Imaging in Mild to Severe Alzheimer Disease

Ropele S, Schmidt R, Enzinger C, Windisch M, Martinez NP, Fazekas F.
AJNR Am J Neuroradiol. 2012

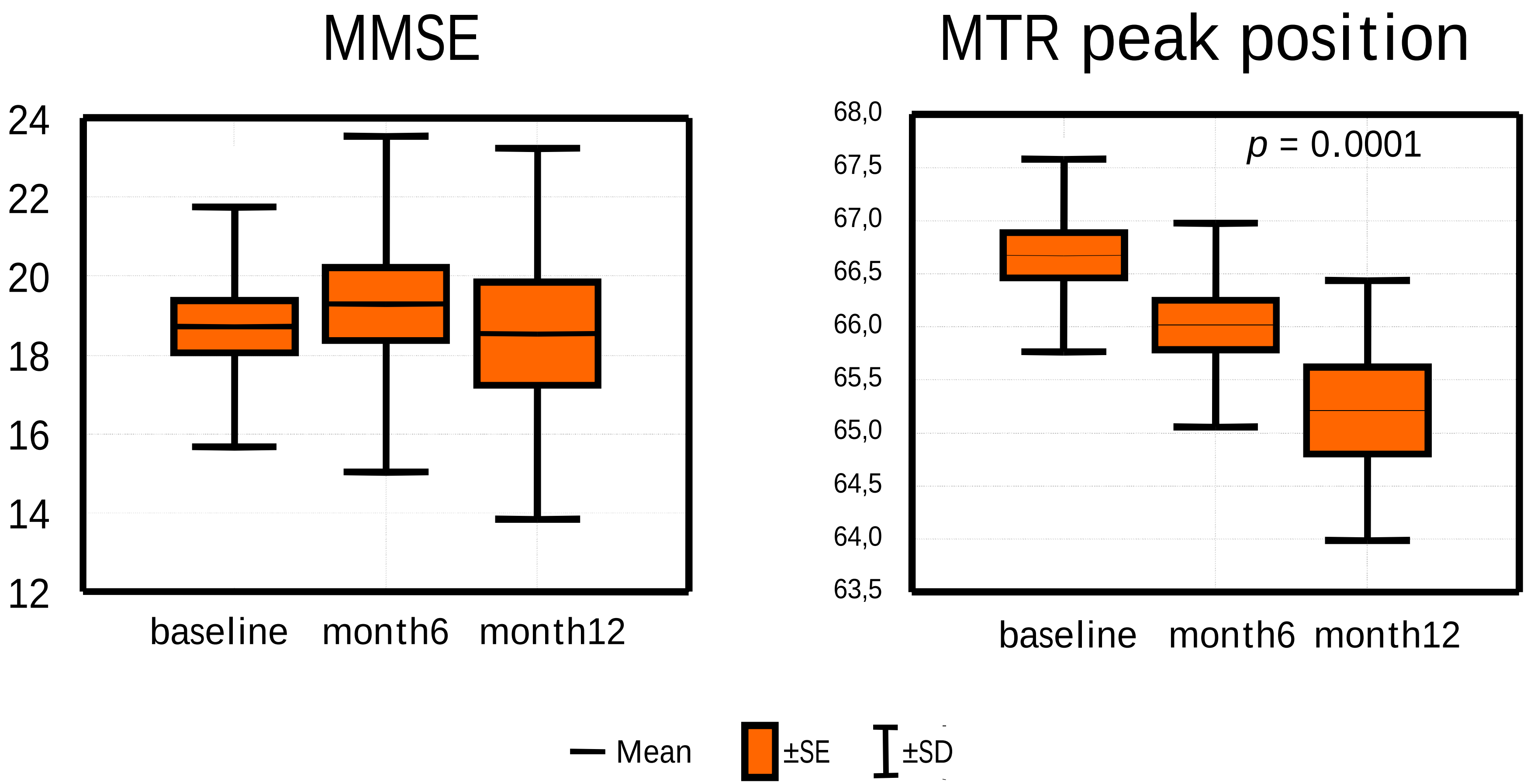

Longitudinal Magnetization Transfer Imaging in Mild to Severe Alzheimer Disease

ORIGINAL RESEARCH

S. Ropele
R. Schmidt
C. Enzinger
M. Windisch
N.P. Martinez
F. Fazekas

Longitudinal analyses of memantine treated vs. placebo subgroups revealed similar results as for the whole AD cohort

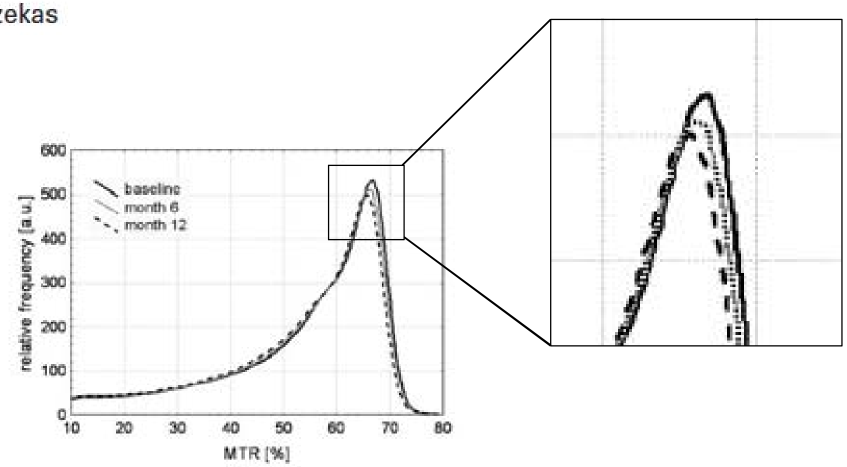

Fig 1. Averaged histograms from all AD patients for baseline and follow-up scans. Already at month 6, a reduction of both the peak position and the relative peak height are clearly visible.

Table 2: Relation between deep gray matter MTR and cognition in AD patients at baseline

	MMSE	
	r	*p*
Left hippocampus	0.57	<0.01
Right hippocampus	0.38	0.048
Left putamen	0.70	<0.001
Right putamen	0.60	<0.01
Left thalamus	0.52	<0.01
Right thalamus	0.42	0.029
Left caudate nucleus	0.07	0.69
Right caudate nucleus	-0.06	0.72

Note:—Stronger correlations can be consistently observed in the left hemisphere.

The Manifold Applications of Iron Tracing

- Quantification of global and regional iron load as an associate of aging and neurodegeneration
- Senile plaque detection in vivo
- Iron labeling to study BBB transport

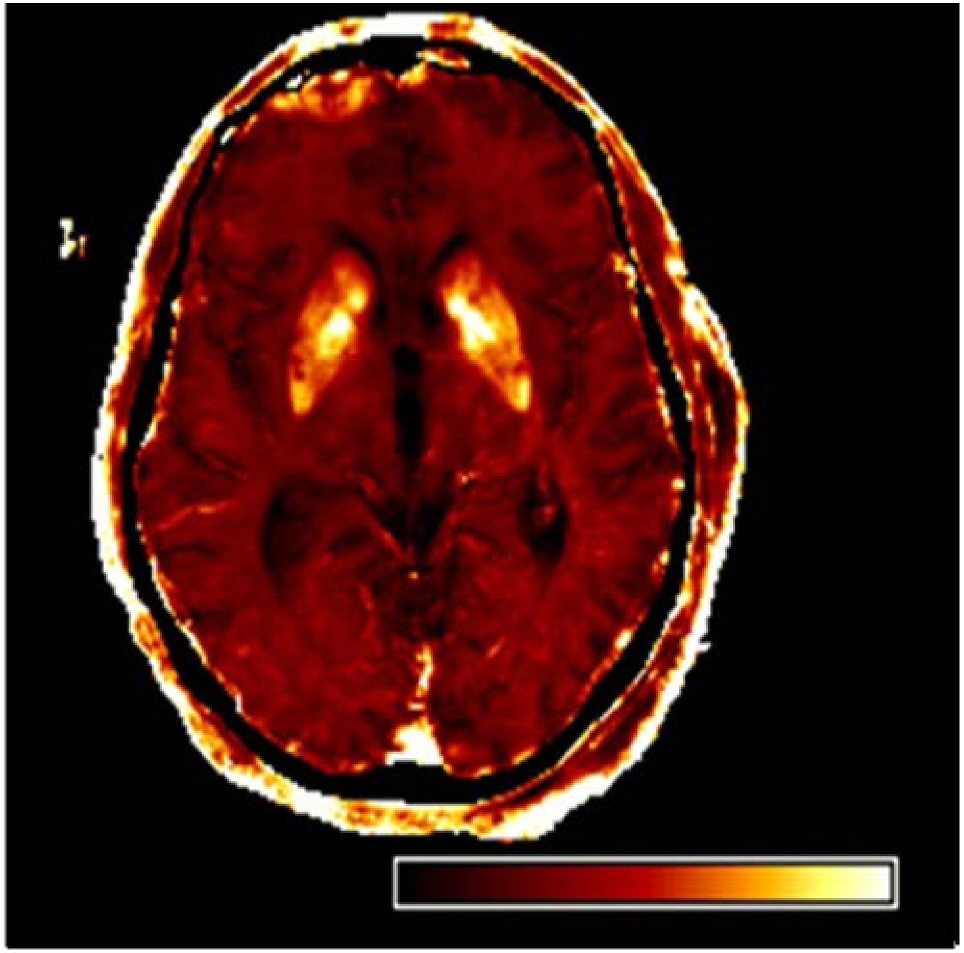

Monitoring treatment effects: Interesting methods with limited data
Microstructural changes Iron content

Iron & the brain

- /?žž?ž?žž?žž?žž?žž?ž?ž?žž?žž?ž reflection rest of body due to BBB
- Distribution iron over the brain ?V uniform
  - Varies over cell types
    - oligodendrocytes > neurons > astrocytes
  - Regional variation
    - motor function-related > non-motor-related areas

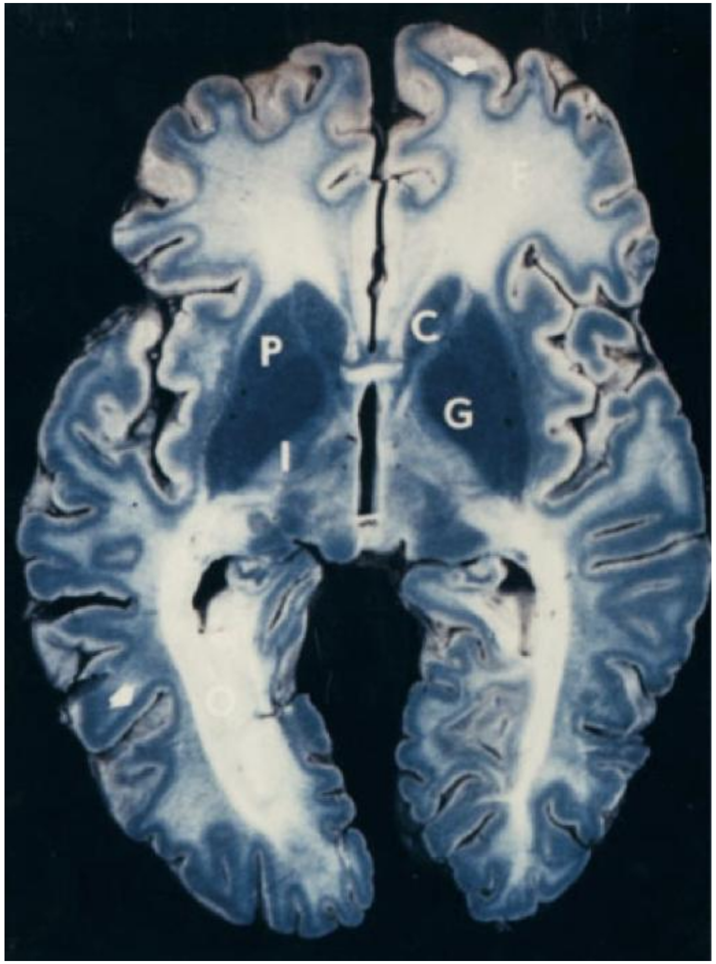

Monitoring treatment effects: Interesting methods with limited data

Microstructural changes Iron content

Iron & the brain

- Iron progressively accumulates with age
- Iron-induced oxidative stress can cause neurodegeneration
- Increasing evidence that iron accumulation is involved in many brain disorders

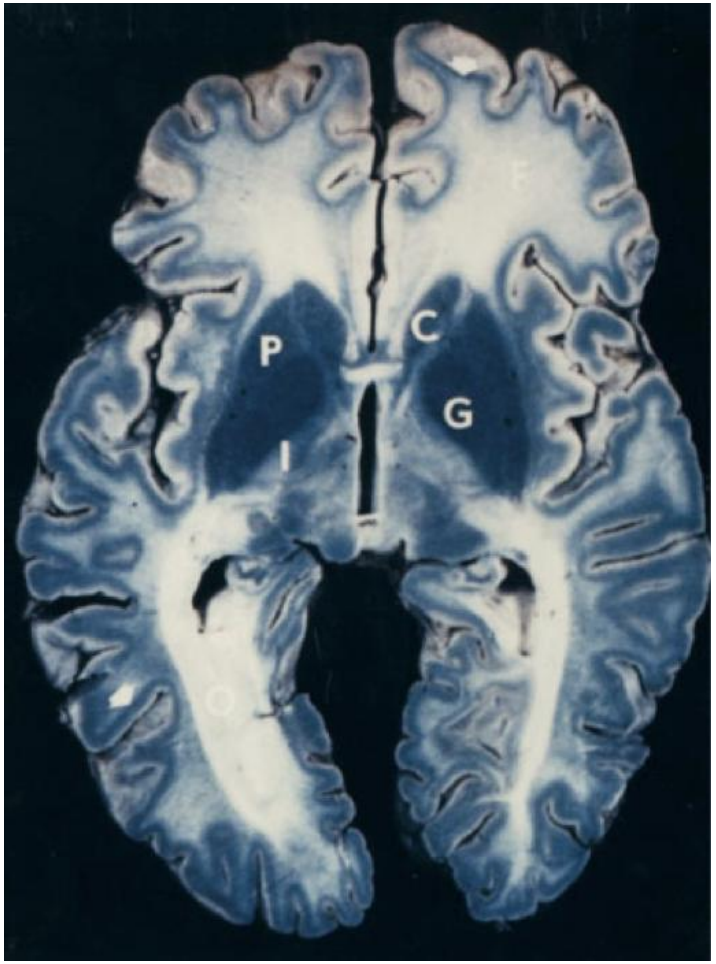

Iron accumulates with age and relates to brain disease

normal accumulation:

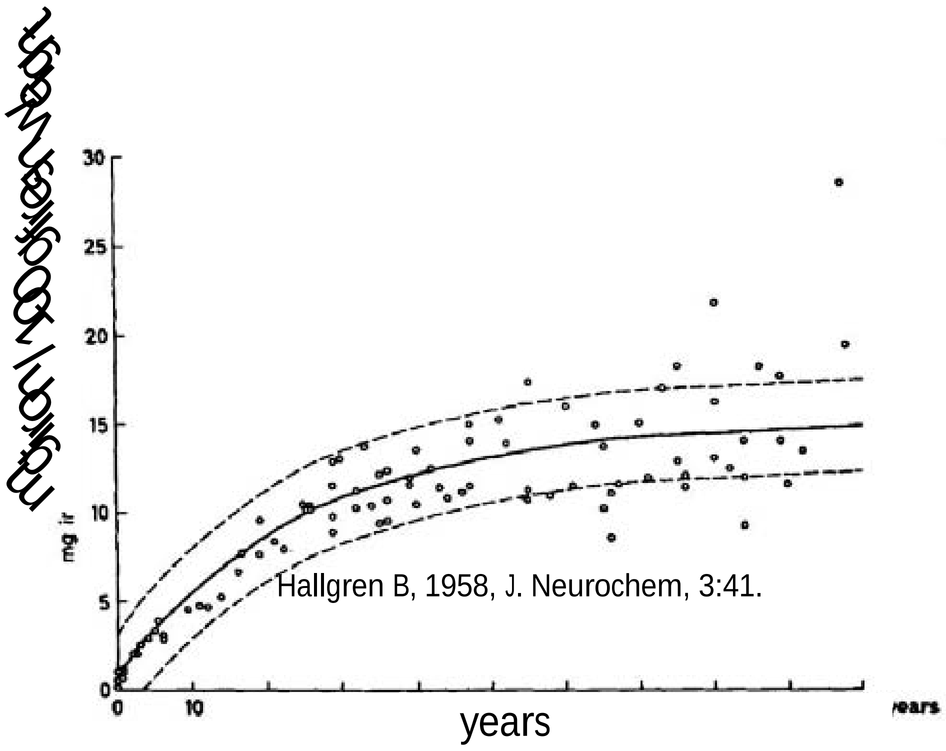

Hallgren B, 1958, J. Neurochem, 3:41.

abnormal accumulation in:

- Huntington‘s disease (HD)
- Parkinson‘s disease (PD)
- Alzheimer‘s disease (AD)
- Multiple sclerosis (MS)
- Chronic hemorrhage
- Cerebral infarction
- Down syndrome
- AIDS

Age-related changes in the brain

Age-related iron accumulation

MRI manifestations - old age: patterns

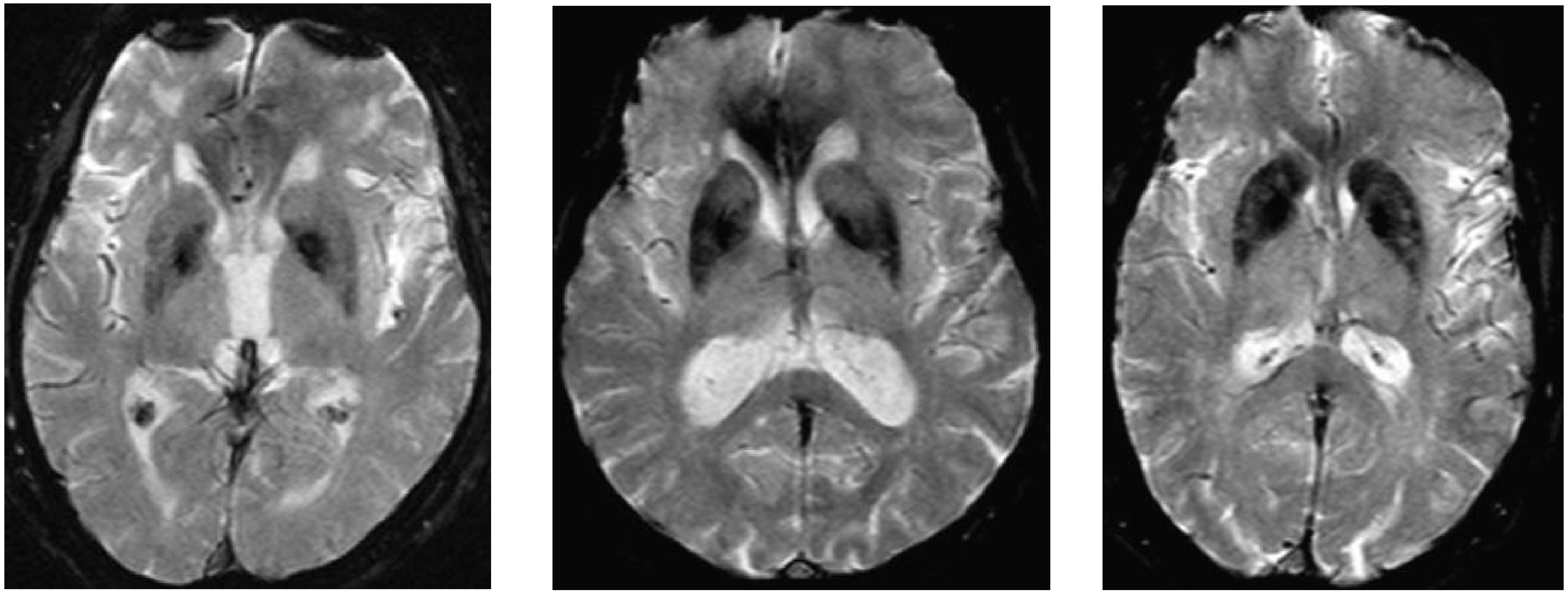

The Manifold Applications of Iron Tracing

- Quantification of global and regional iron load as an associate of aging and neurodegeneration
- Senile plaque detection in vivo
- Iron labeling to study BBB transport

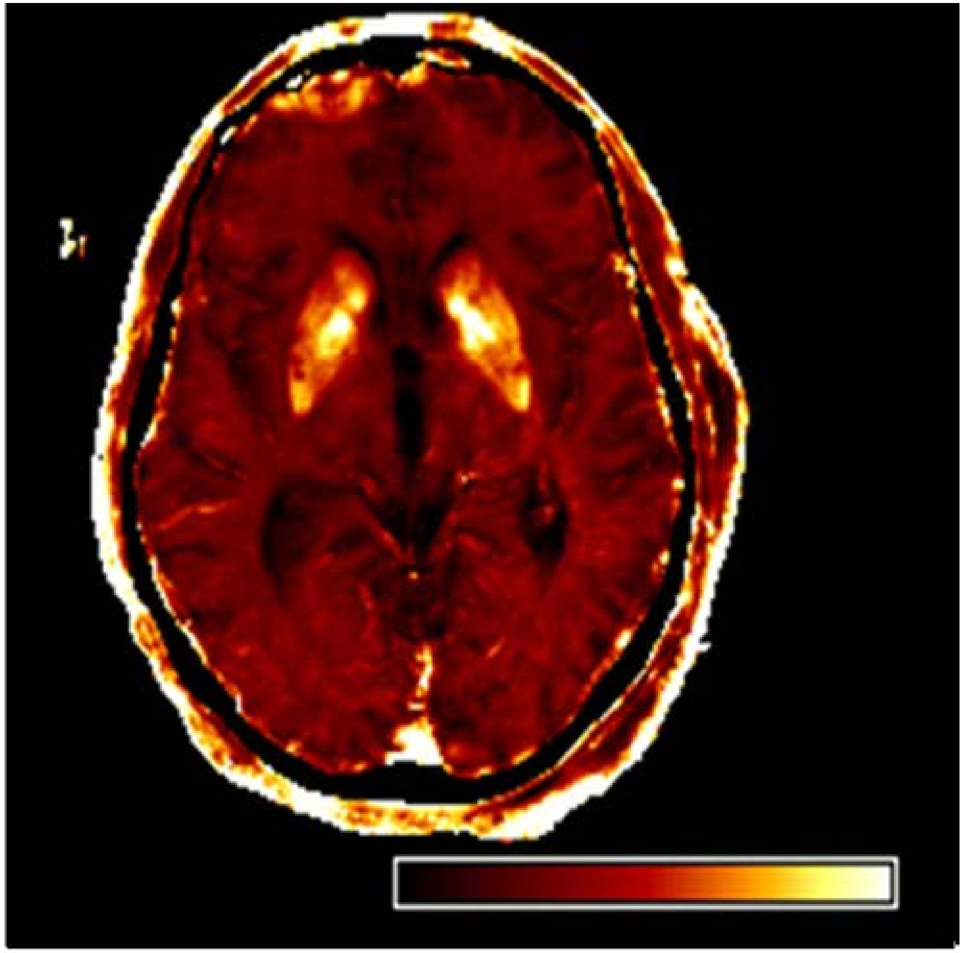

Iron mapping in AD

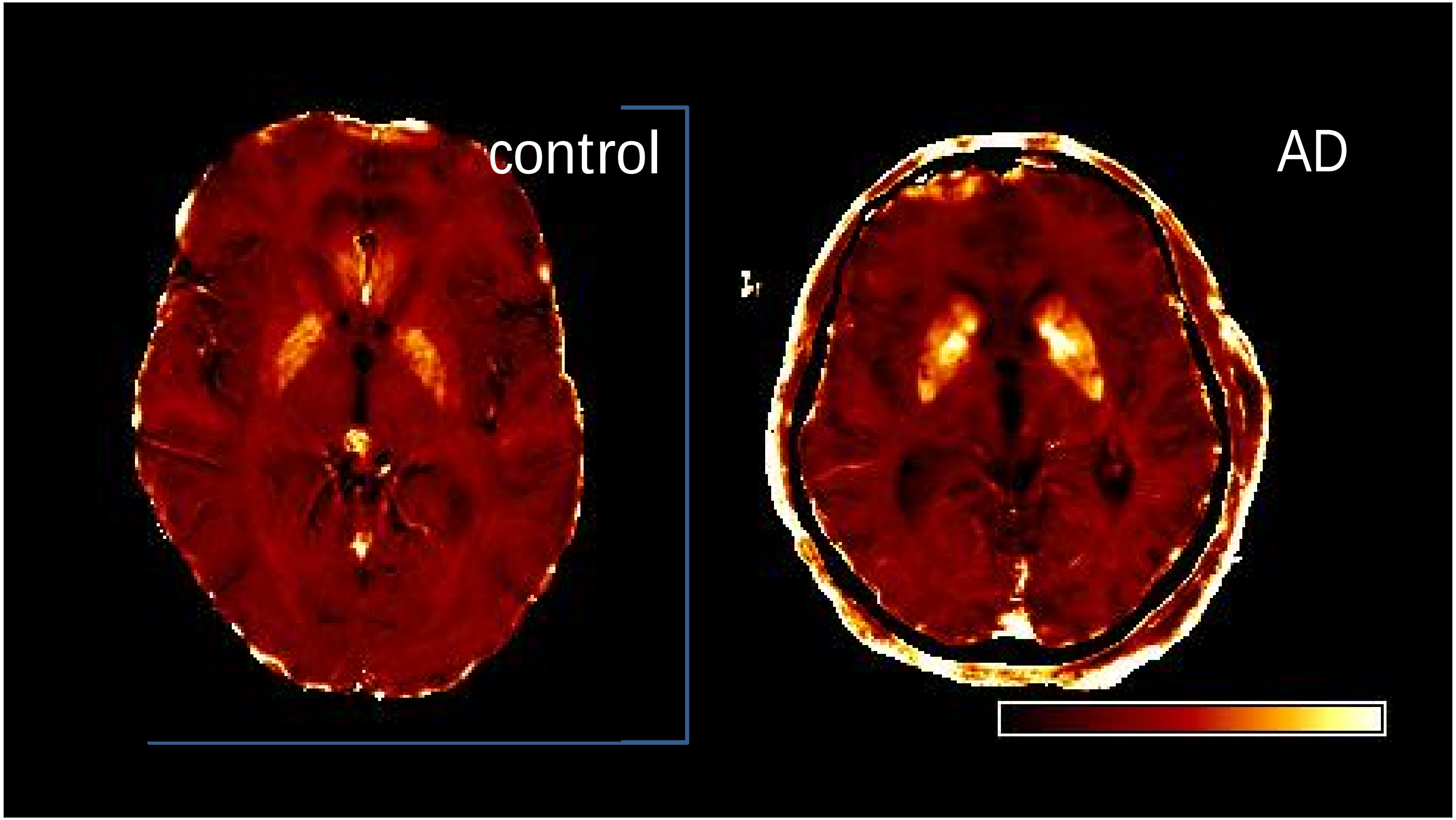

Radiology

ORIGINAL RESEARCH ■ NEURORADIOLOGY

Quantitative MR Imaging of Brain Iron: A Postmortem Validation Study[1]

Christian Langkammer, MSc
Nikolaus Krebs, MD
Walter Goessler, PhD
Eva Scheurer, MD, MSc
Franz Ebner, MD
Kathrin Yen, MD
Franz Fazekas, MD
Stefan Ropele, PhD

[1] From the Department of Neurology (C.L., F.F., S.R.) and Division of Neuroradiology, Department of Radiology (F.E.), Medical University of Graz, Auenbruggerplatz 22, 8036 Graz, Austria; Ludwig Boltzmann Institute for Clinical Forensic Imaging, Graz, Austria (C.L., N.K., E.S., K.Y.); and Institute of Chemistry-Analytical Chemistry, University of Graz, Graz, Austria (W.G.). Supported by the Austrian Science Fund (project P20103-B02). Received March 5, 2010; revision requested April 19; revision received June 7; accepted June 16; final version accepted June 28. Address correspondence to S.R. (e-mail: *stefan.ropele@medunigraz.at*).

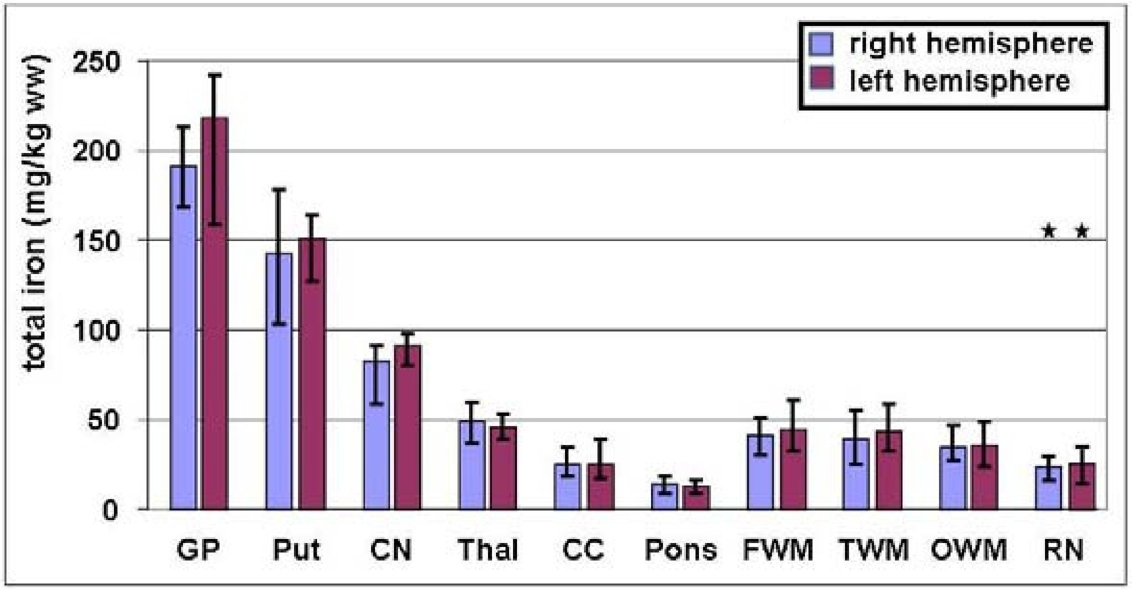

Iron

Iron accumulation

Increased iron accumulation in basal ganglia and hippocampus in AD

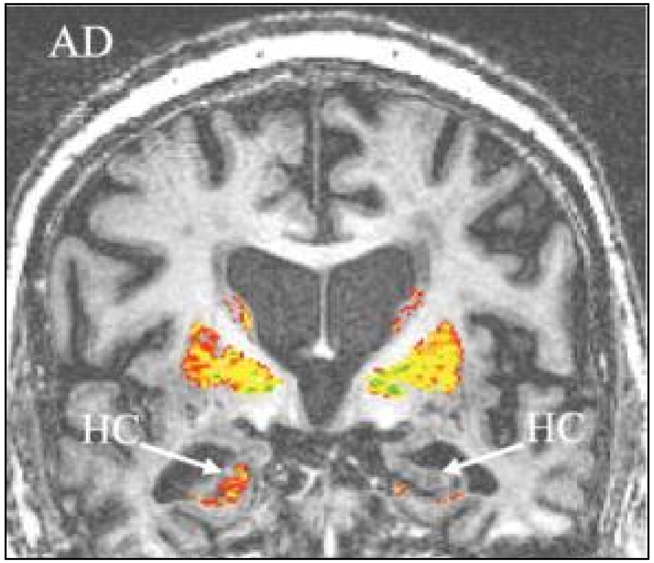

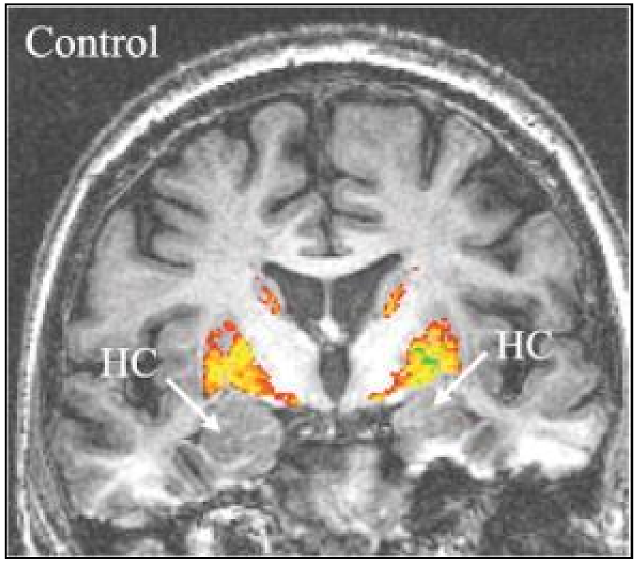

JF Schenck et al., Top Magn Reson Imaging 2007

Iron Accumulation in AD

Zhu W et al, *Radiology* 2009, 253:

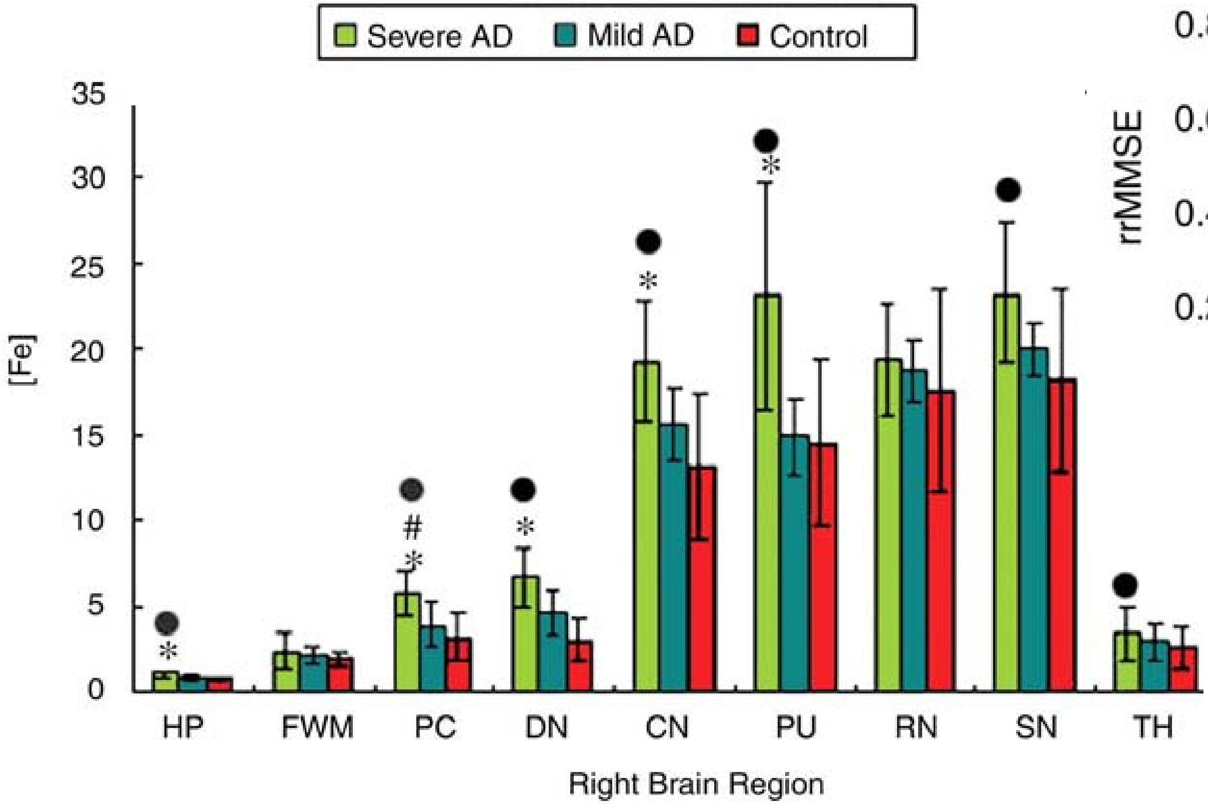

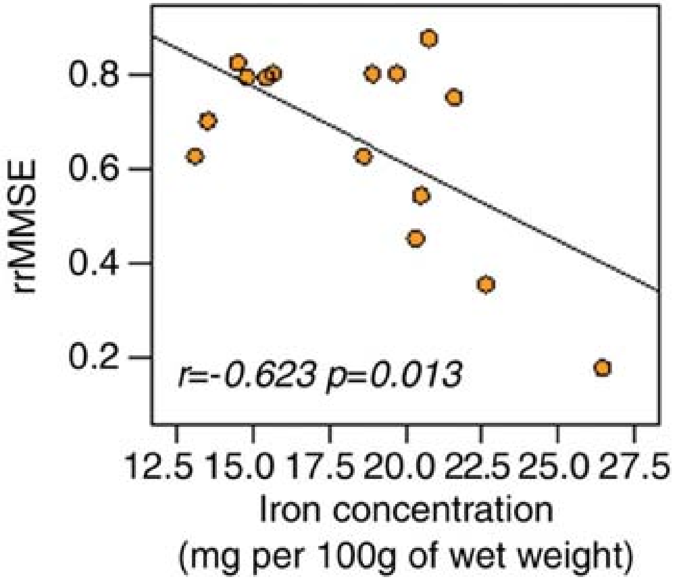

Phase data: the basis for qSM

$$\varphi = \gamma \Delta B * TE$$

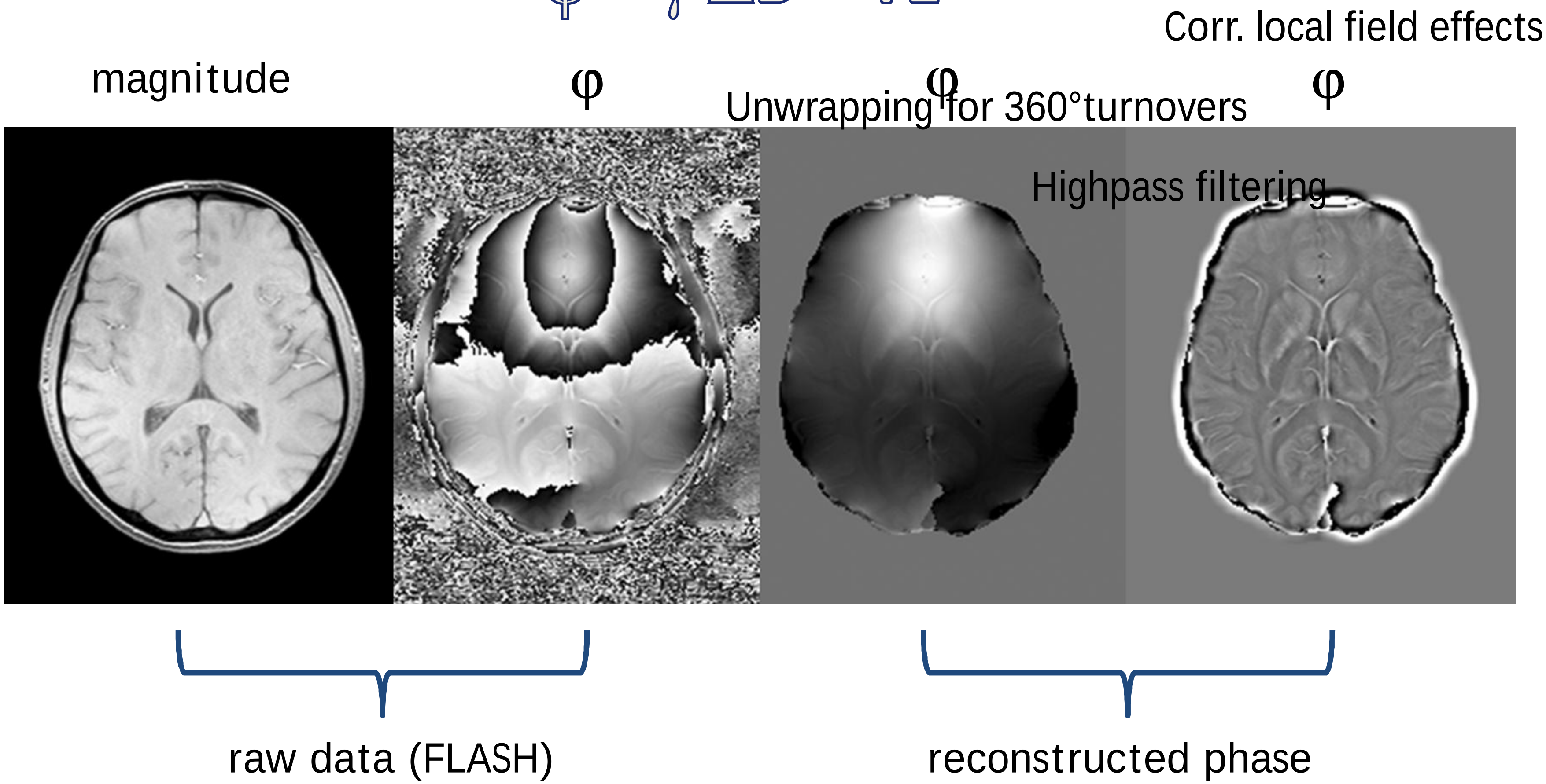

qSM in AD

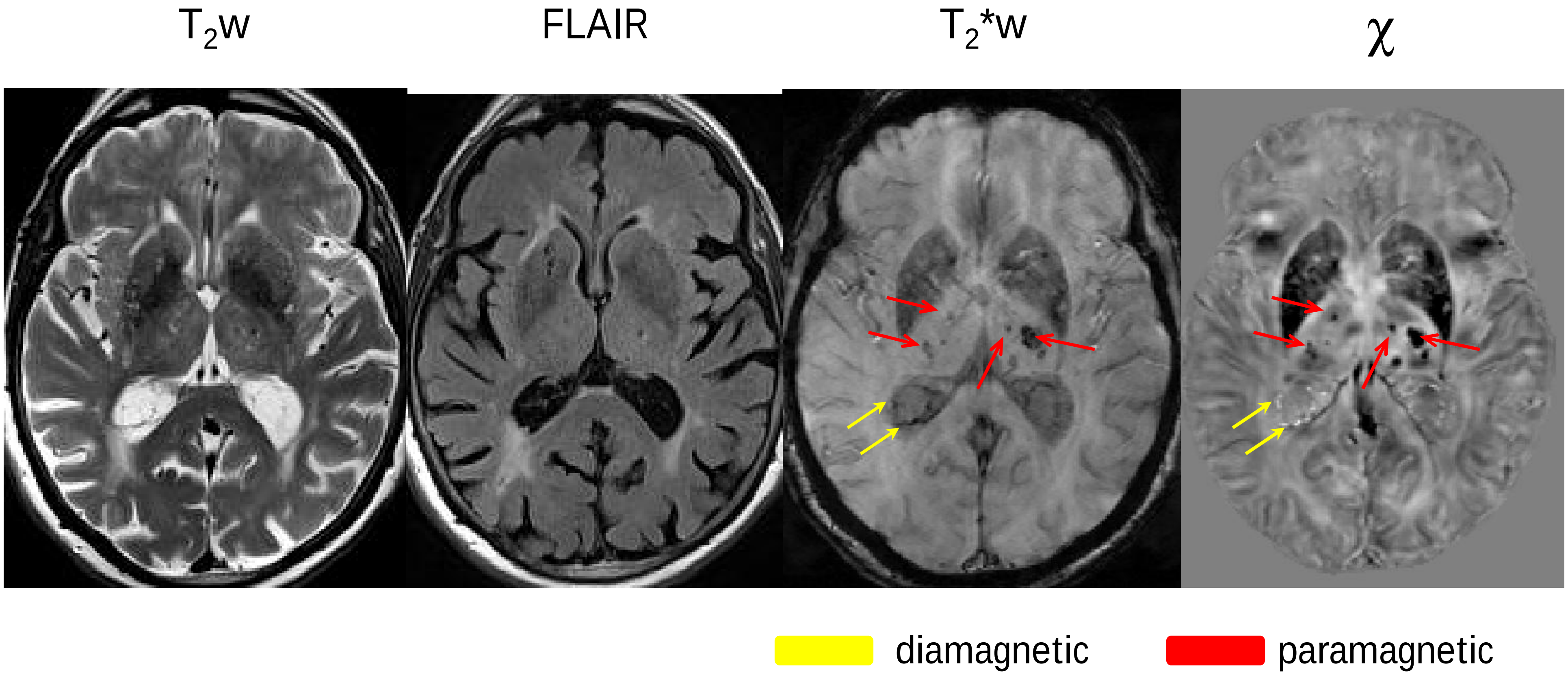

MEDI reconstruction of 3D FLASH data

Postmortem validation of qSM @3T

13 corpses, 457 specimens

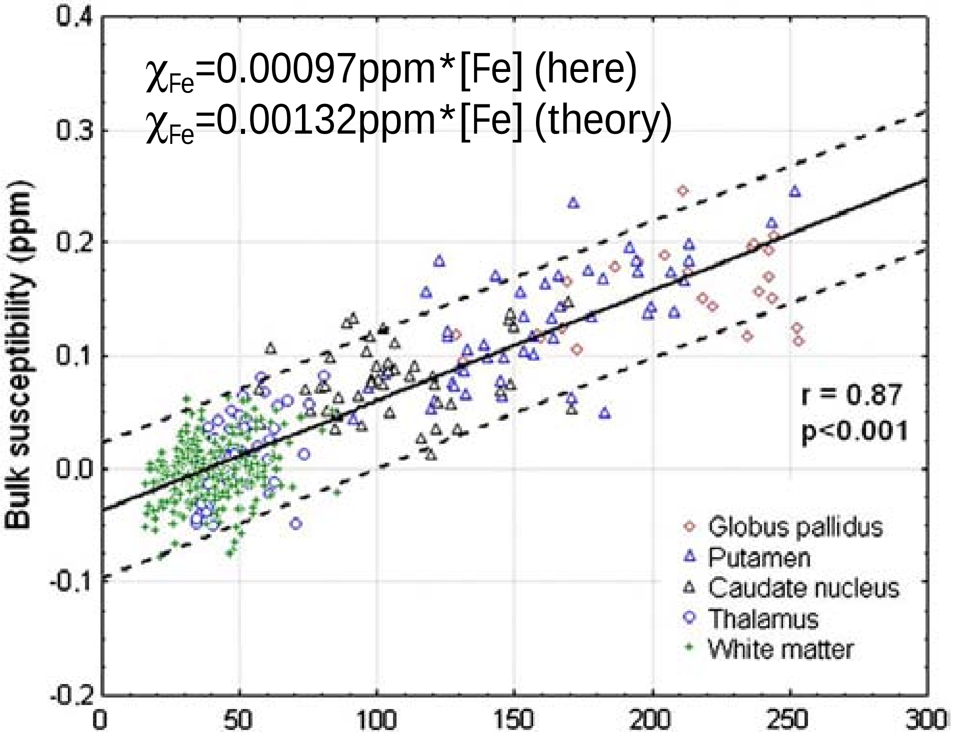

iron concentration (mg/kg wet mass)

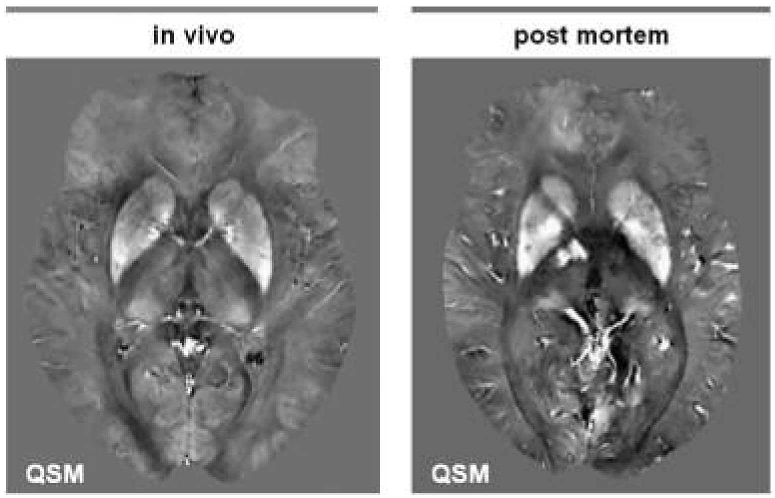

Quantitative susceptibility mapping (QSM) as a means to measure brain iron? A post mortem validation study

Langkammer C et al. Neuroimage 2012

The Manifold Applications of Iron Tracing

- Quantification of global and regional iron load as an associate of aging and neurodegeneration
- Senile plaque detection in vivo
- Iron labeling to study BBB transport

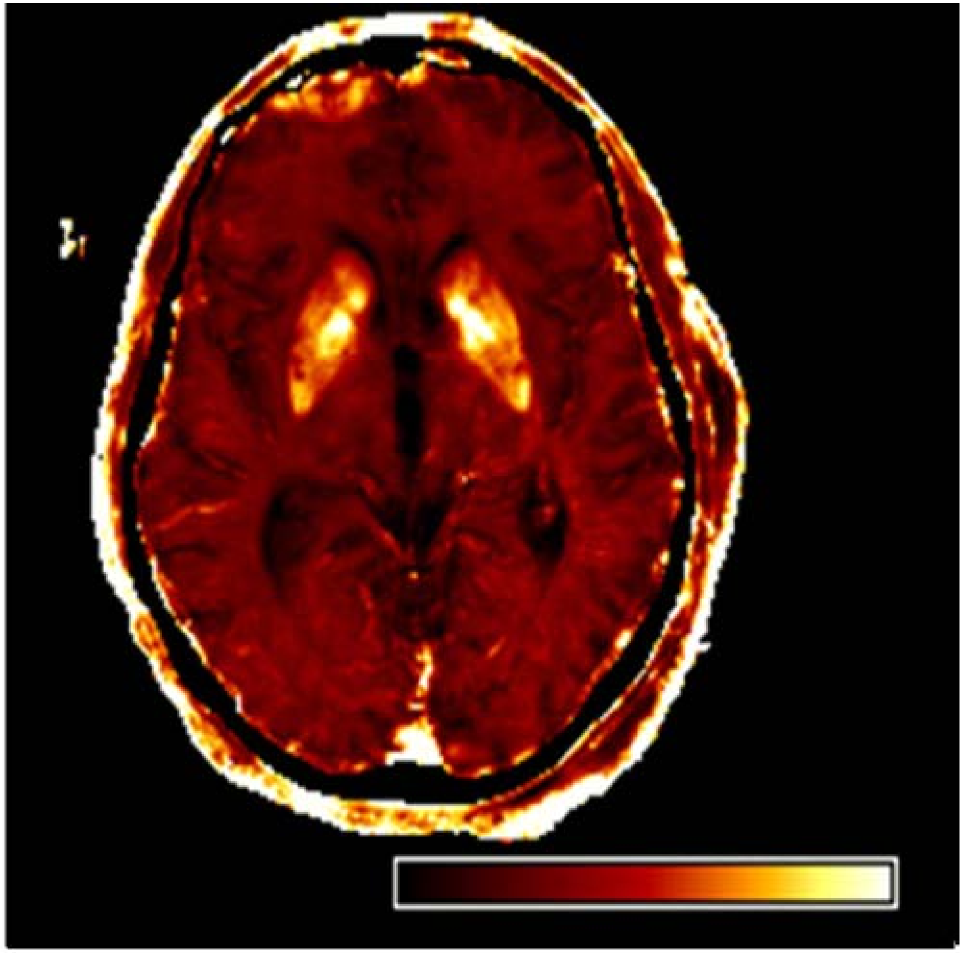

Specific iron accumulation in AD

§ Iron deposition at AD specific brain sites (HC, amygdala, cortex)

Cornett et al. Neurotoxicology 1998;19:339. Bartzokis G et al. Arch Gen Psychiatry 2000;57:47

§ NFT and SP show accumulated iron

Sayre LM et al. J Neurochem. 2000;74:270. Collingwood JF et al. J Alzheimers Dis. 2005;7:267.

§ A binds iron -> facilitate aggregation of the protein

Garzon-Rodriguez W. Bioorg Med Chem Lett. 1999;9:2243.

Iron in Plaques in the Cortex –Humans

Human ex vivo material @ 7 Tesla (human system)

S. van Rooden et al, Radiology 2009

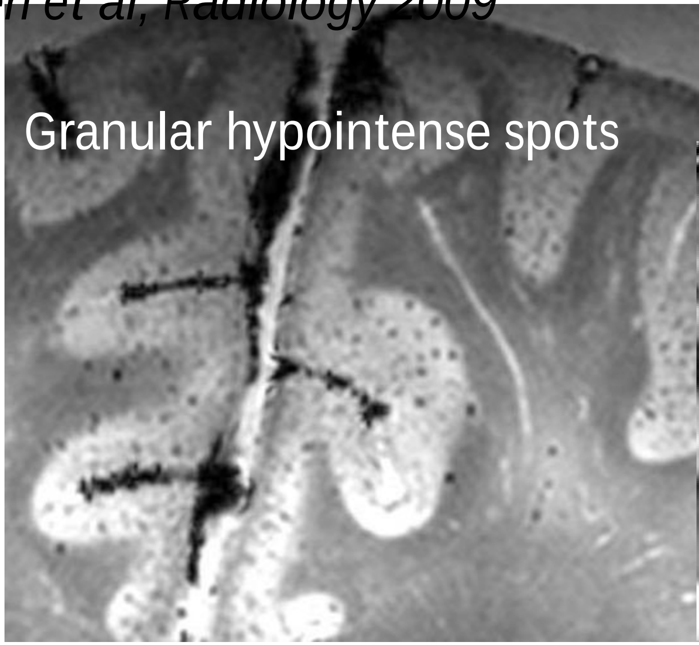

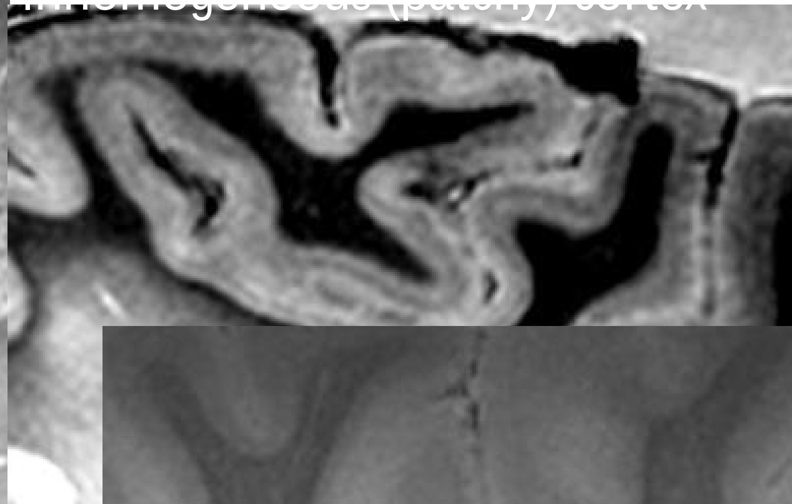

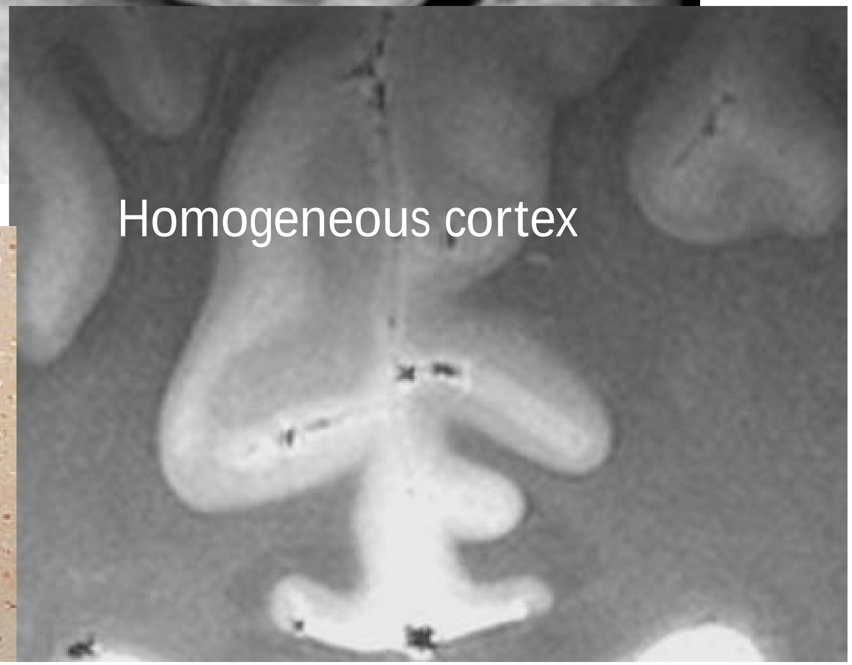

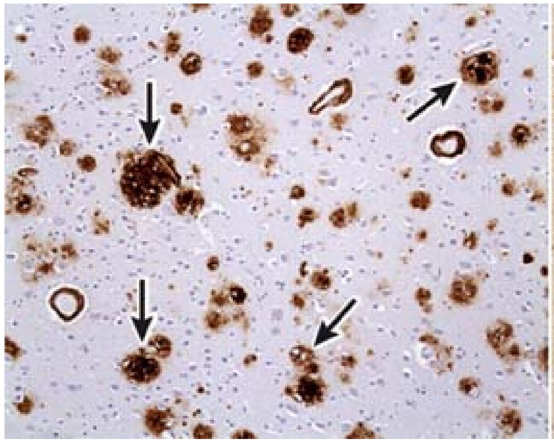

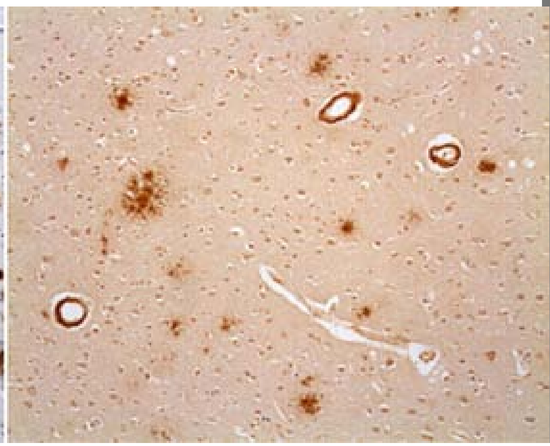

MRI of amyloid plaques

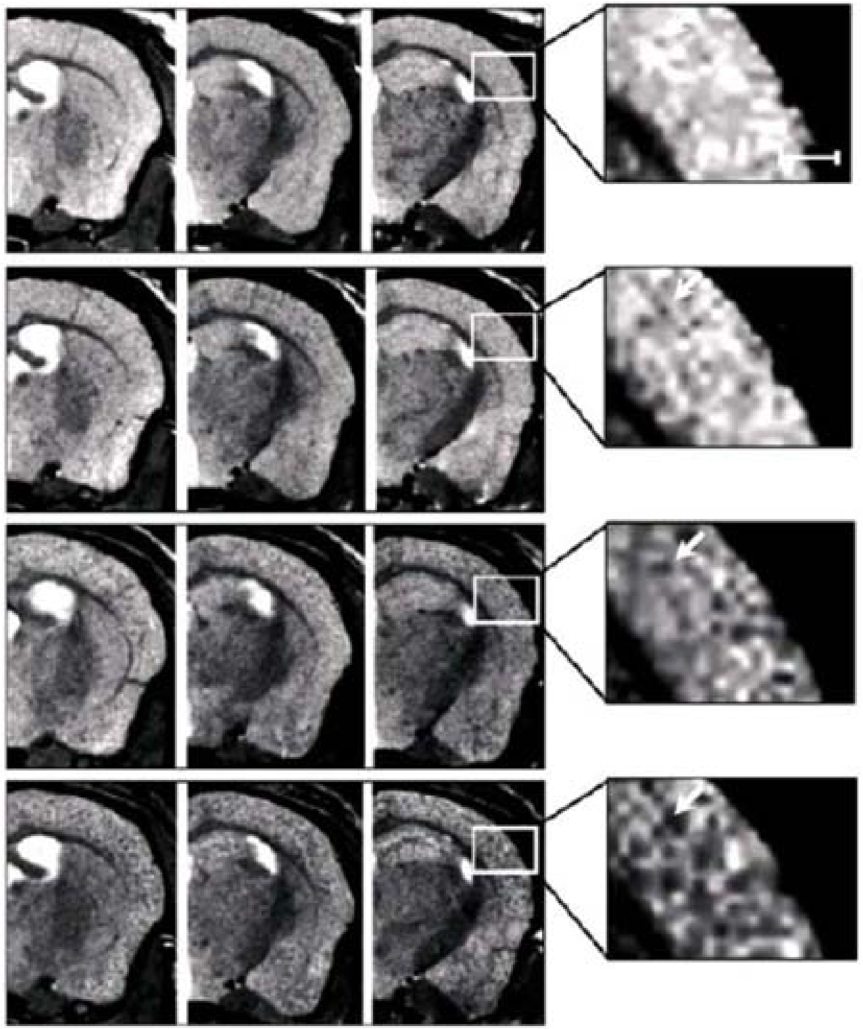

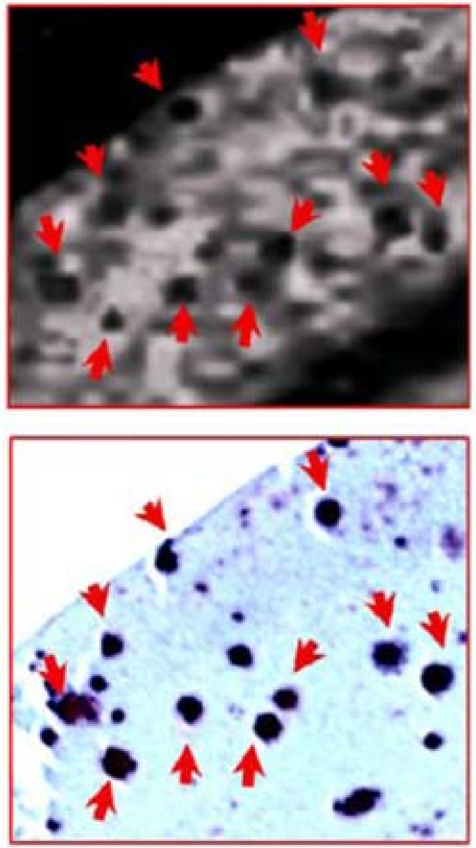

Braakman N et al. JMRI 2006

Pathologically confirmed intracortical infarcts detected by HR-MRI.

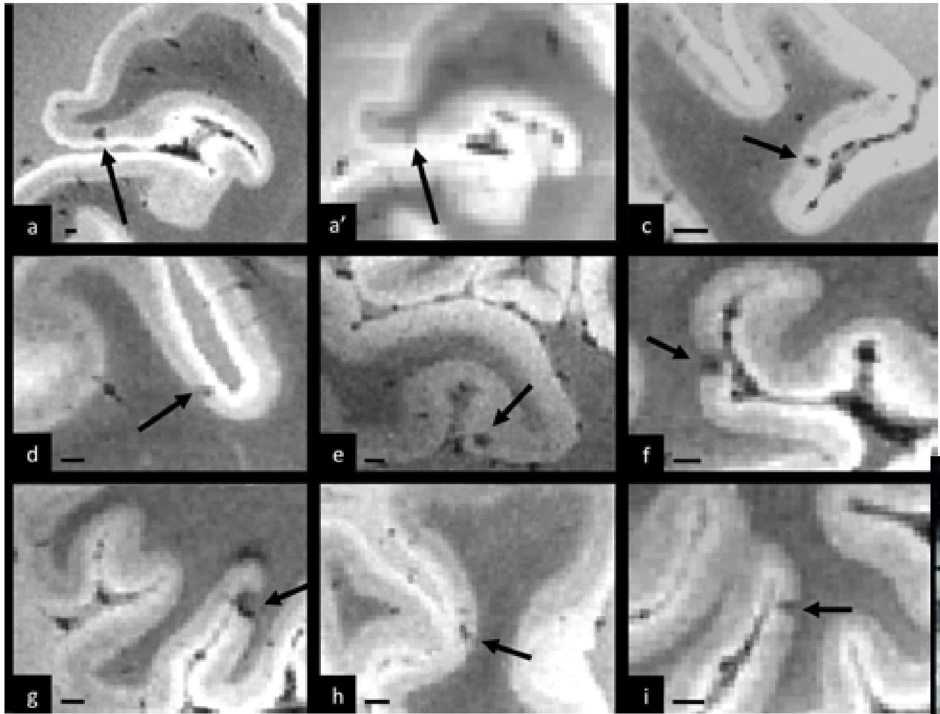

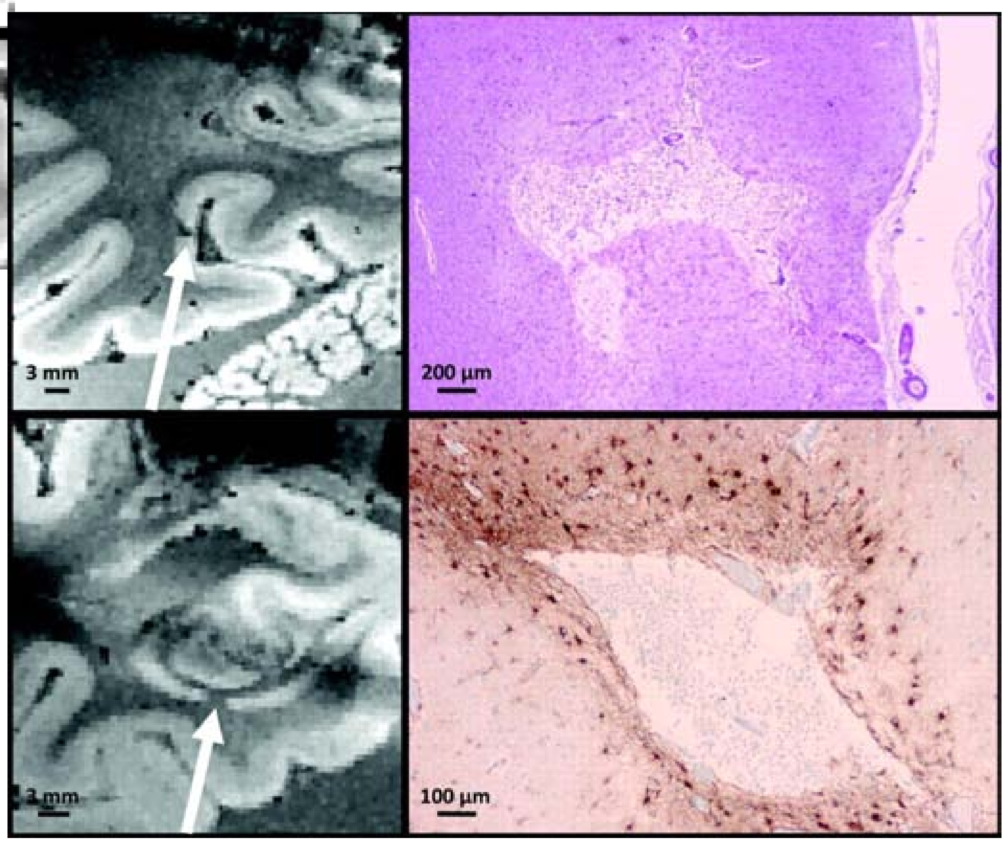

Jouvent E et al. Stroke 2011;42:e27-e30

Journal of Cerebral Blood Flow & Metabolism (2013) 33, 322–329

www.jcbfm.com

FEATURE ARTICLE

In vivo detection of cerebral cortical microinfarcts with high-resolution 7T MRI

Susanne J van Veluw[1], Jaco JM Zwanenburg[2], JooYeon Engelen-Lee[3], Wim GM Spliet[3], Jeroen Hendrikse[2], Peter R Luijten[2] and Geert Jan Biessels[1]

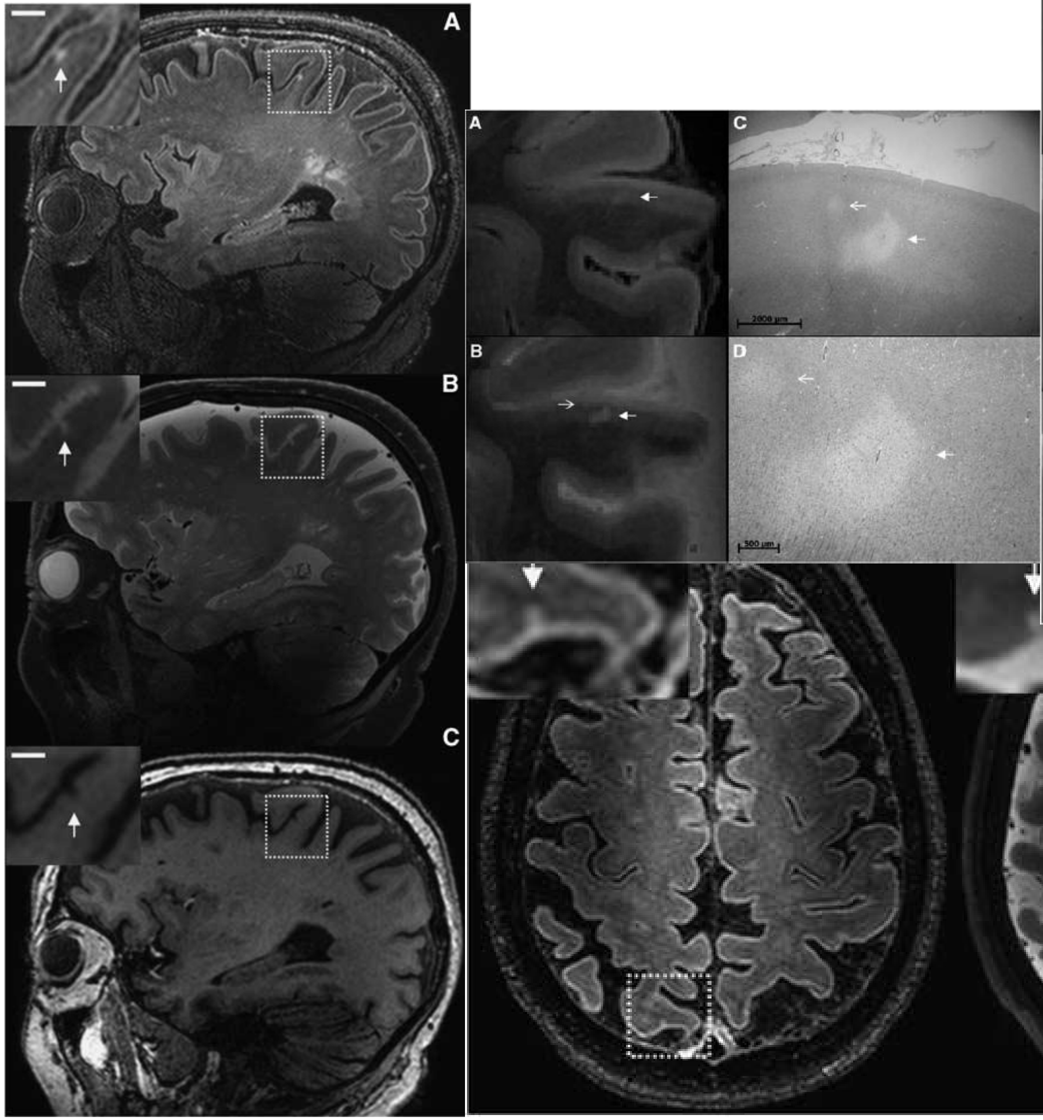

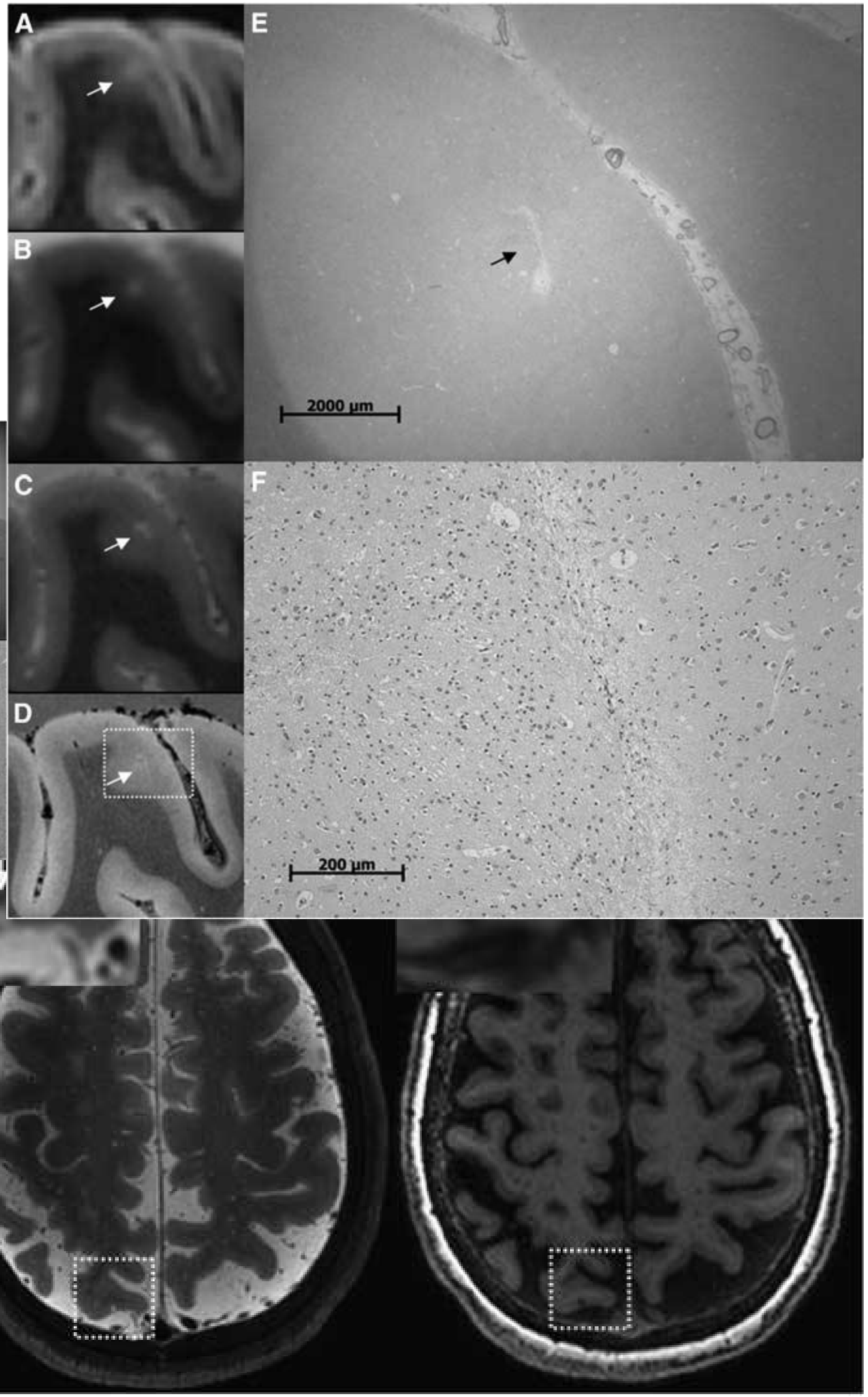

The Manifold Applications of Iron Tracing

- Quantification of global and regional iron load as an associate of aging and neurodegeneration
- Senile plaque detection in vivo
- Iron labeling to study BBB transport

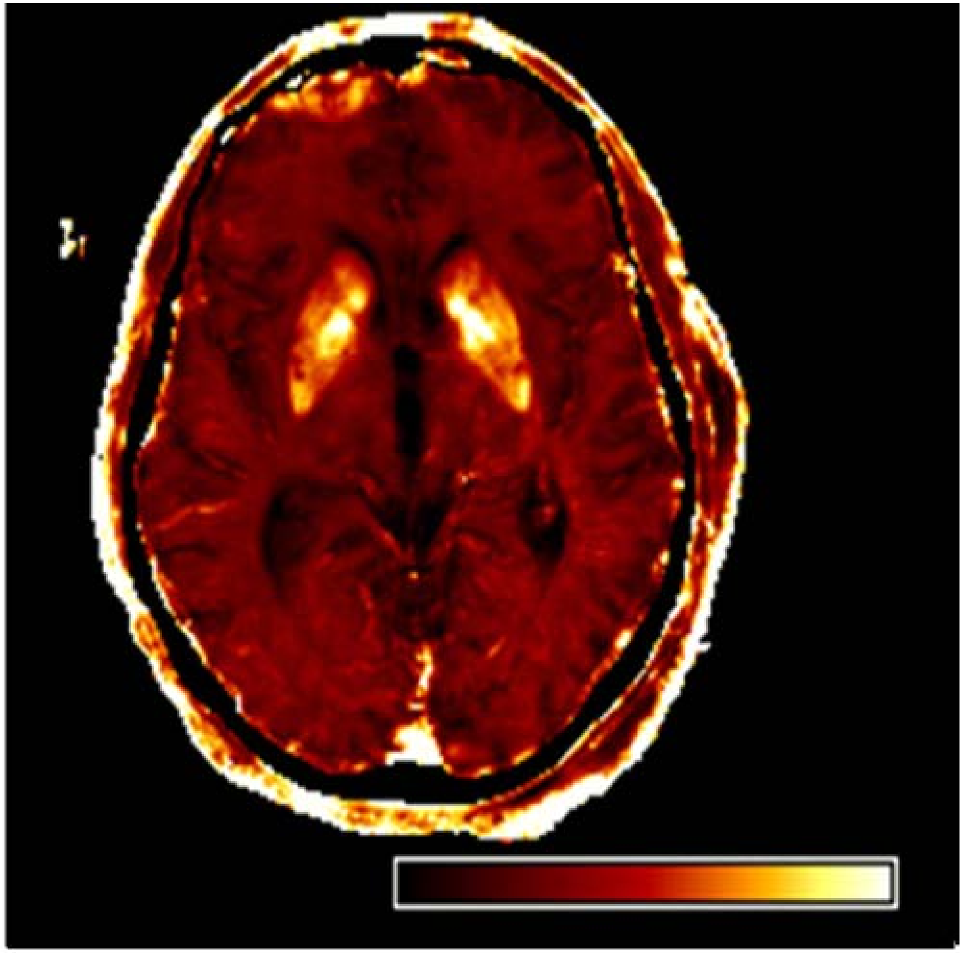

Nanobrain project (ERA-NET call)

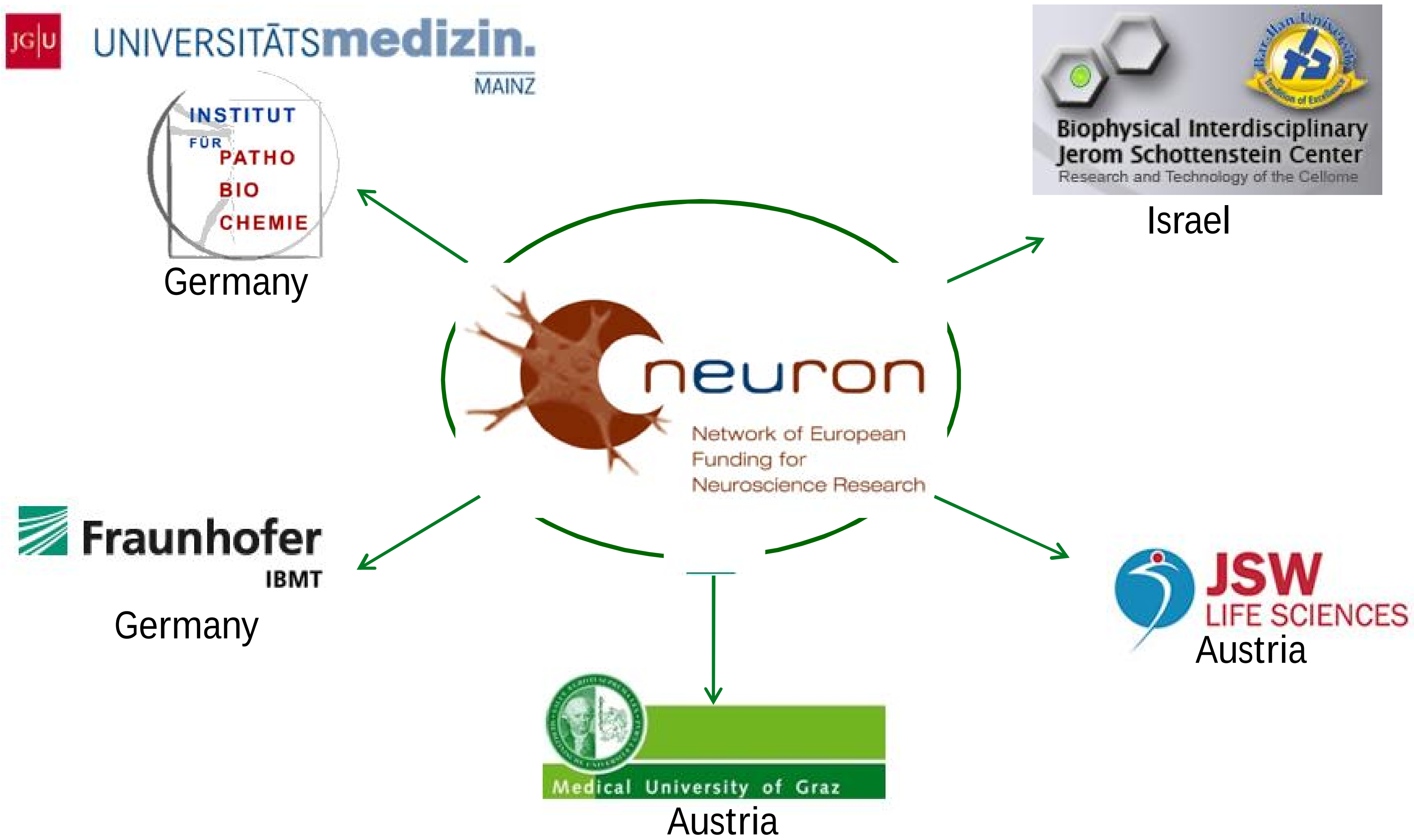

Nanobrain project

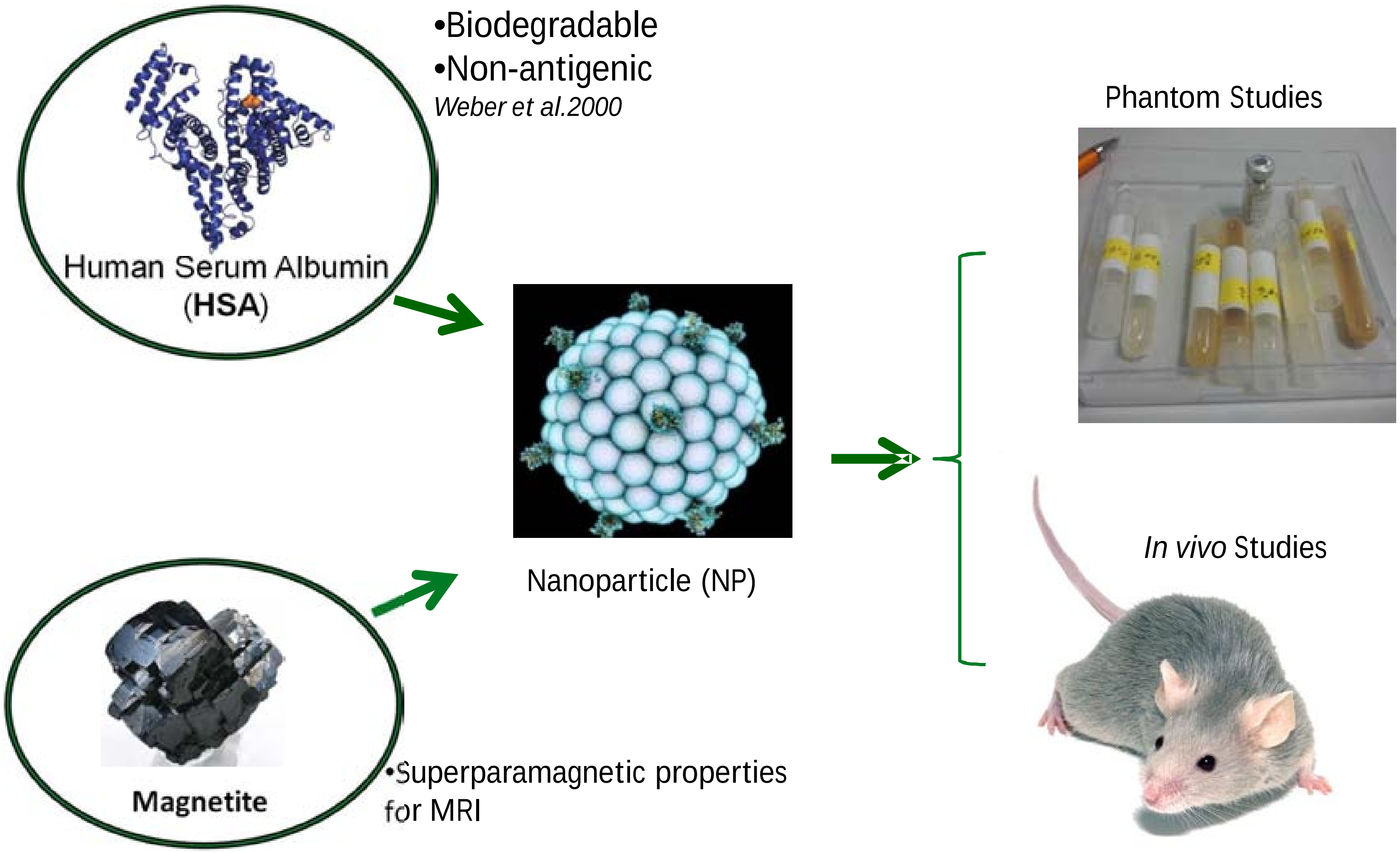

NP uptake in the rat body

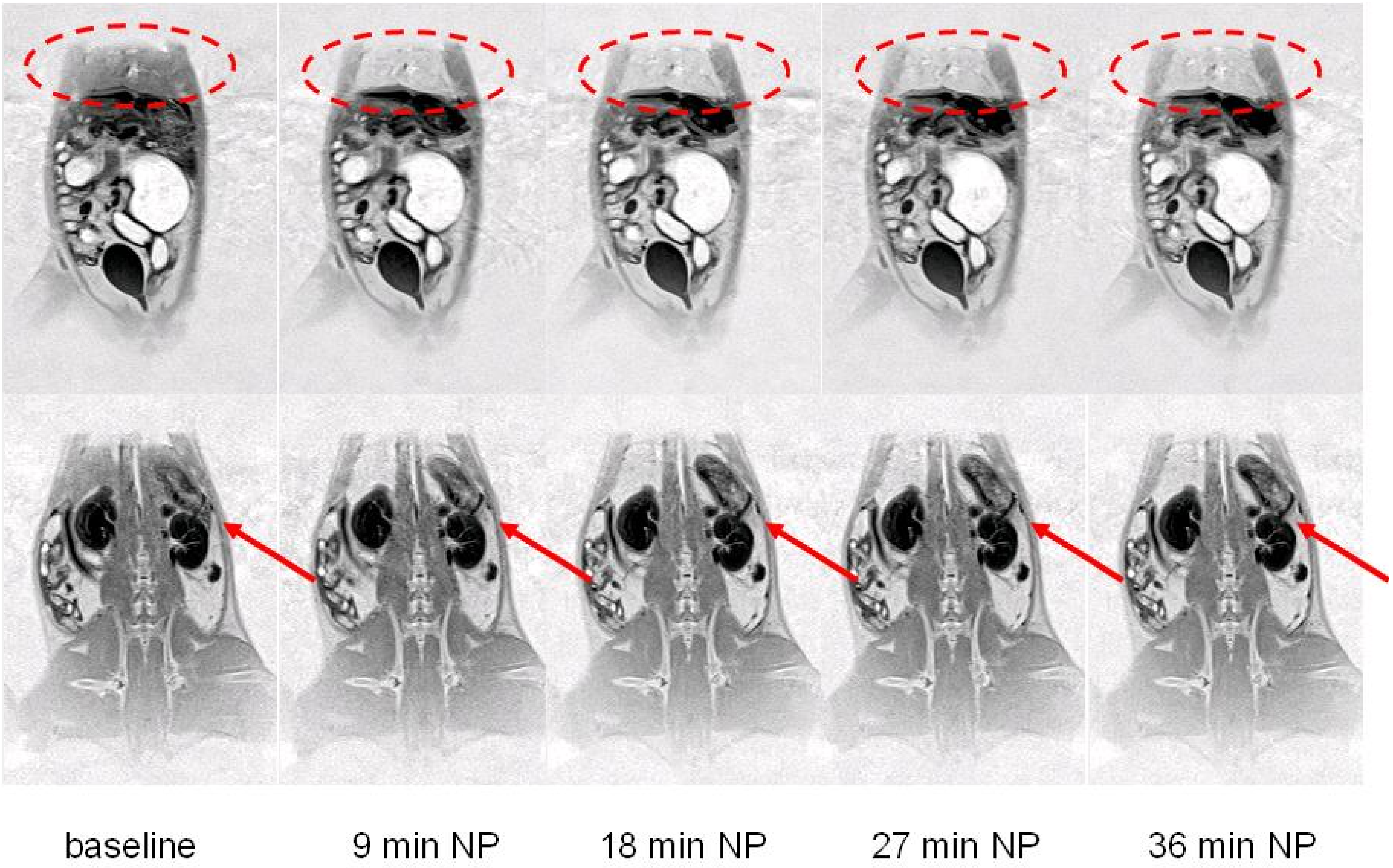

Phase-sensitive IR sequence

T_1 histogram from segmented brain

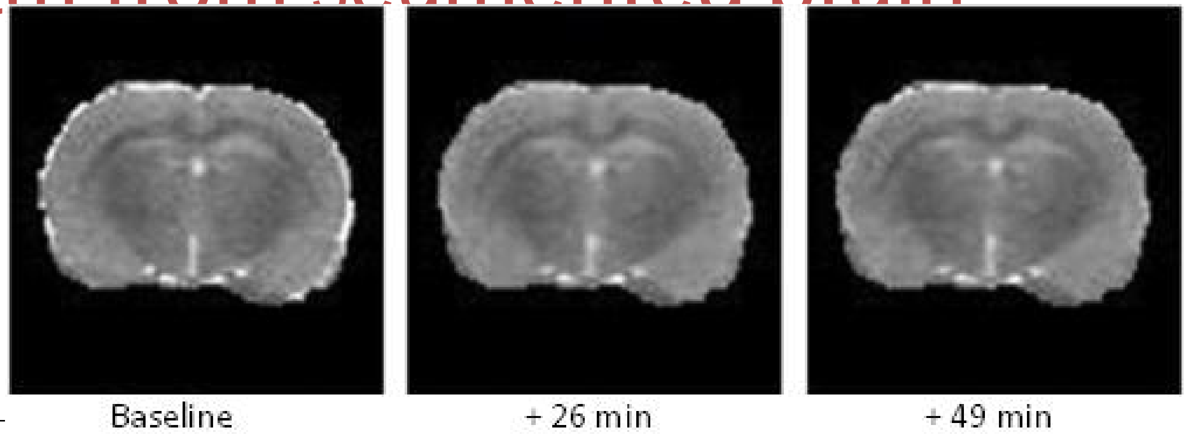

T1 map

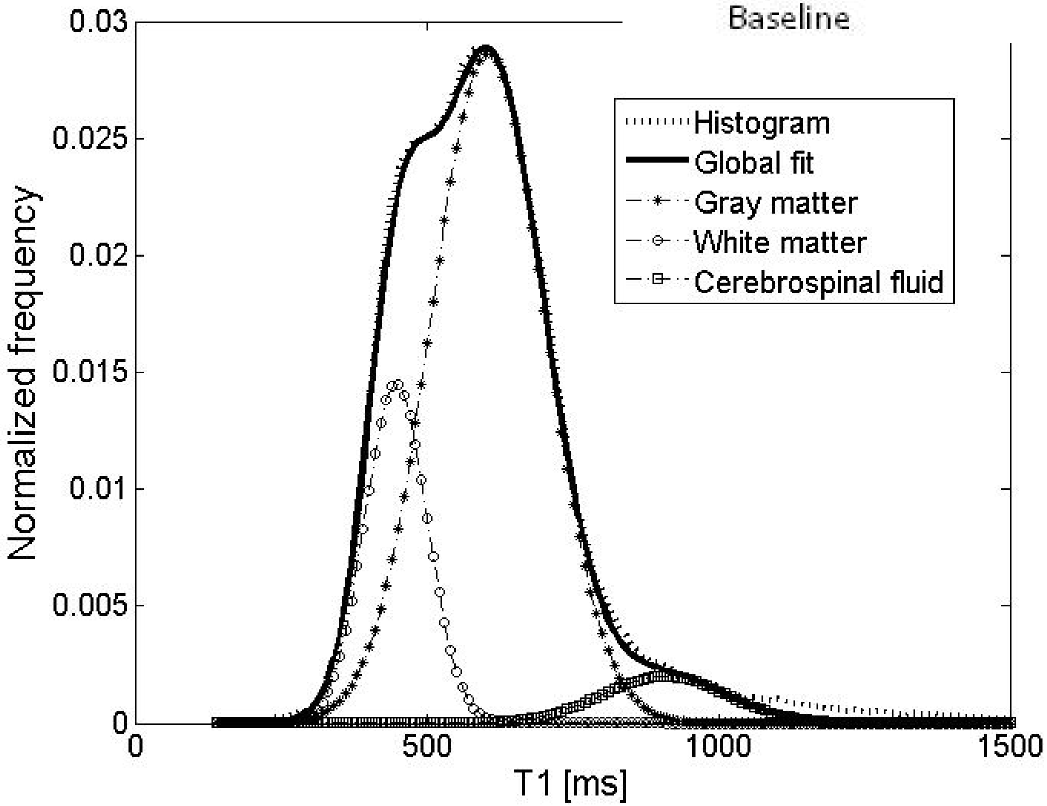

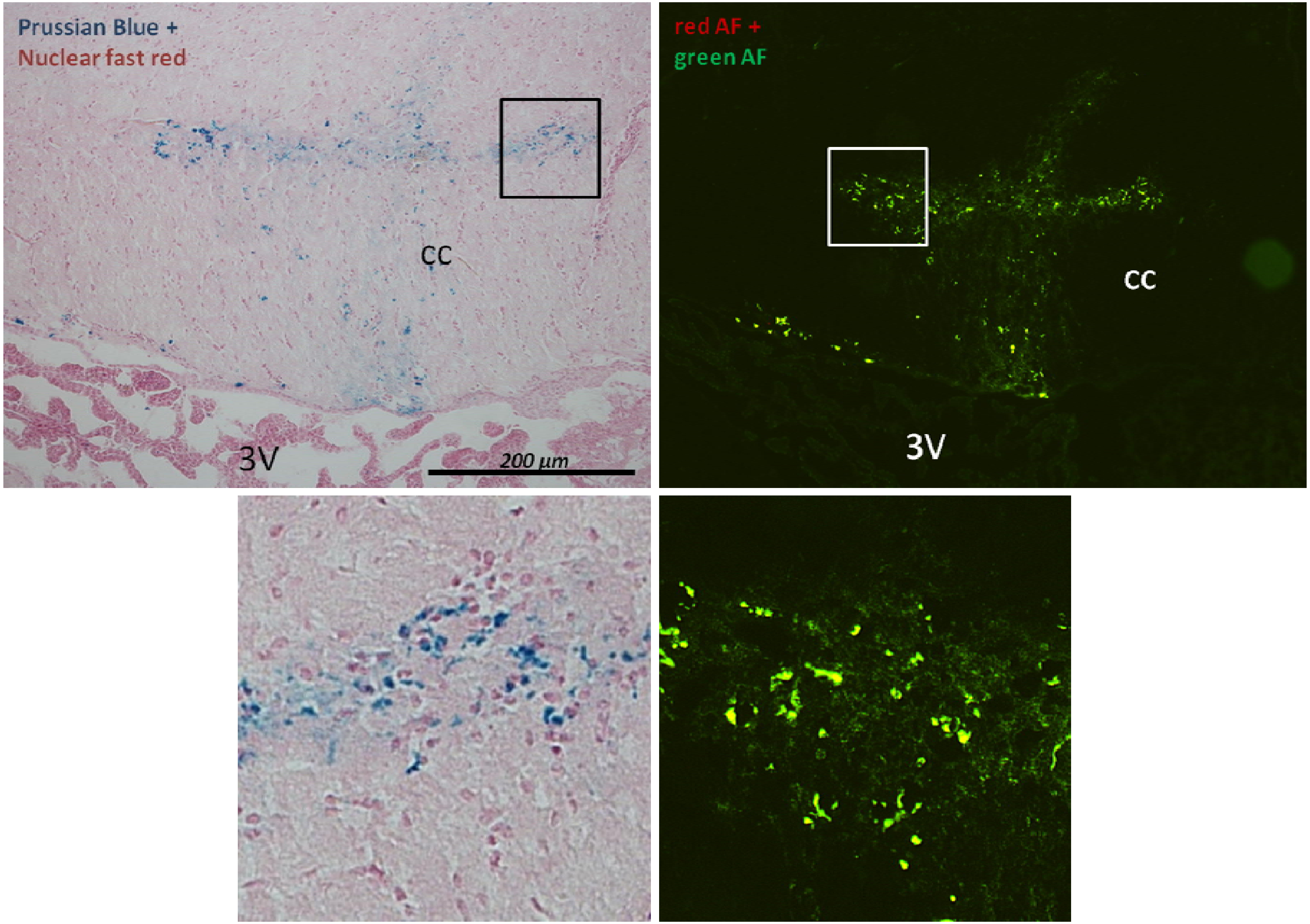
Prussian Blue +
Nuclear fast red
cc
3V
200 µm
red AF +
green AF
cc
3V

MRI versus autofluorescence

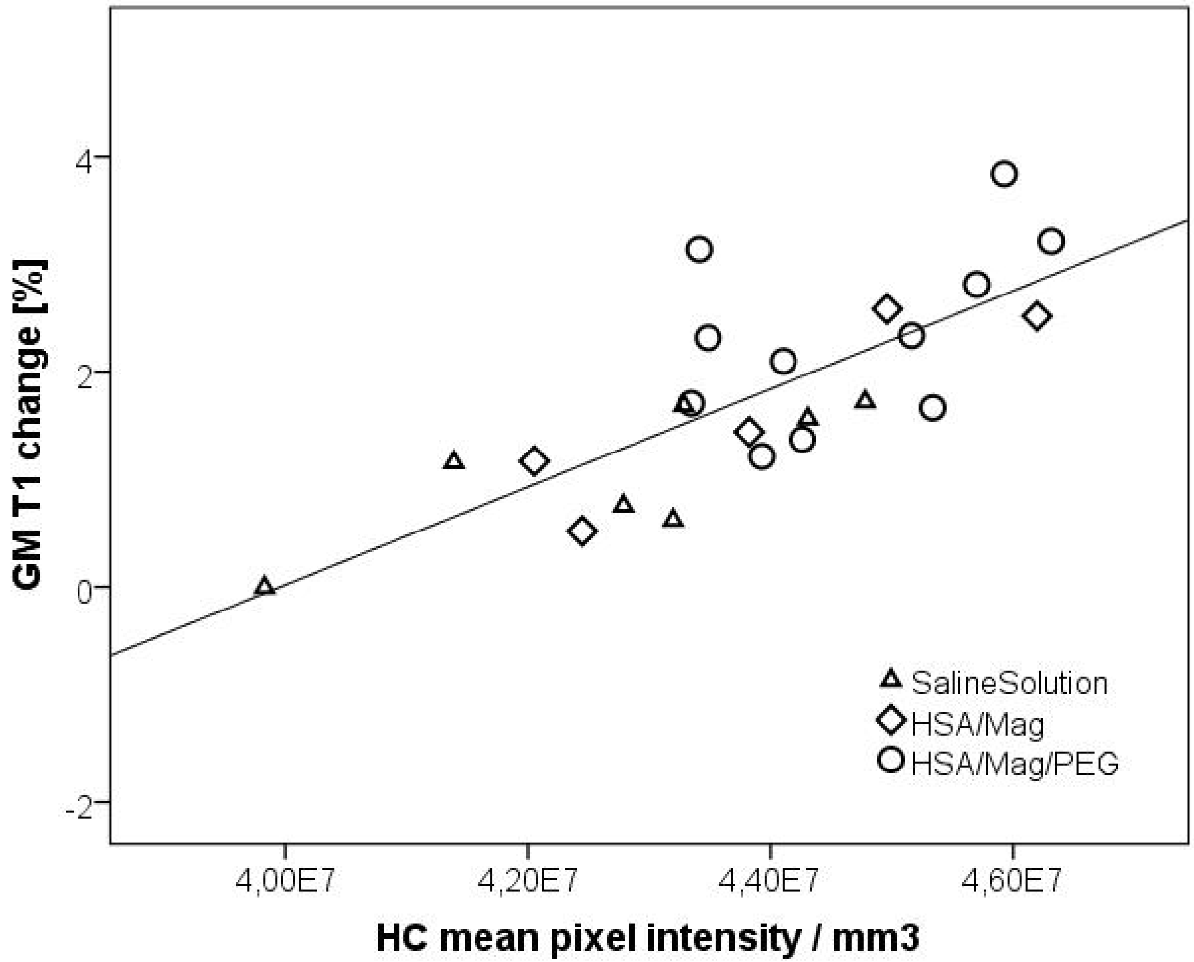

R=0.74, p<0.01

Advanced MRI Techniques allow the in vivo view below the surface

We only start to understand

- underlying tissue pathology
- rate and determinants of progression over time

&

- clinical meaning of different metrics